International Ocean Discovery Program
Expedition 366 Scientific Prospectus

Mariana serpentinite mud volcanism: geochemical, tectonic, and biological processes

Patricia Fryer
Co-Chief Scientist
Hawaii Institute of Geophysics and Planetology
University of Hawaii
1680 East–West Road
Honolulu Hawaii 96821
USA

C. Geoffrey Wheat
Co-Chief Scientist
University of Alaska, Fairbanks
PO Box 475
Moss Landing CA 95039
USA

Trevor Williams
Expedition Project Manager/Staff Scientist
International Ocean Discovery Program
Texas A&M University
1000 Discovery Drive
College Station TX 77845-9547
USA

IODP
INTERNATIONAL OCEAN DISCOVERY PROGRAM

Publisher's notes

This publication was prepared by the *JOIDES Resolution* Science Operator (JRSO) at Texas A&M University (TAMU) as an account of work performed under the International Ocean Discovery Program (IODP). Funding for IODP is provided by the following international partners:

National Science Foundation (NSF), United States
Ministry of Education, Culture, Sports, Science and Technology (MEXT), Japan
European Consortium for Ocean Research Drilling (ECORD)
Ministry of Science and Technology (MOST), People's Republic of China
Korea Institute of Geoscience and Mineral Resources (KIGAM)
Australia-New Zealand IODP Consortium (ANZIC)
Ministry of Earth Sciences (MoES), India
Coordination for Improvement of Higher Education Personnel, Brazil (CAPES)

Portions of this work may have been published in whole or in part in other IODP documents or publications.

This IODP *Scientific Prospectus* is based on precruise *JOIDES Resolution* Facility advisory panel discussions and scientific input from the designated Co-Chief Scientists on behalf of the drilling proponents. During the course of the cruise, actual site operations may indicate to the Co-Chief Scientists, the Staff Scientist/Expedition Project Manager, and the Operations Superintendent that it would be scientifically or operationally advantageous to amend the plan detailed in this prospectus. It should be understood that any proposed changes to the science deliverables outlined in the plan presented here are contingent upon the approval of the IODP JRSO Director.

Disclaimer

Copyright

Citation

Fryer, P., Wheat, C.G., and Williams, T., 2016. *Expedition 366 Scientific Prospectus: Mariana Serpentine Mud Volcanism.* International Ocean Discovery Program. http://dx.doi.org/10.14379/iodp.sp.366.2016

ISSN

World Wide Web: 2332-1385

April 2016

Abstract

International Ocean Discovery Program (IODP) Expedition 366 has two primary science objectives. The first objective is devoted to coring a series of sites at the summit and flanks of three large (up to 50 km diameter and 2 km high) serpentinite mud volcanoes in the Mariana forearc (within 100 km west of the Mariana Trench). This objective addresses the broad scientific aim of examining processes of mass transport within the subduction zone of a nonaccretionary convergent margin. In detail, the plan is to recover mudflow materials to (1) examine processes of mass transport and geochemical cycling within the forearc of a nonaccretionary convergent margin; (2) ascertain the spatial variability of slab-related fluids within the forearc environment as a means of tracing dehydration, decarbonation, and water-rock reactions in subduction and suprasubduction zone environments; (3) study the metamorphic and tectonic history of this nonaccretionary forearc region; (4) investigate the physical properties of the subduction zone in relation to dehydration reactions and seismicity; (5) document microbial activity associated with subduction zone material from great depth; and (6) explore linkages among these subduction-related processes, including seismicity, while placing the effects of these processes within a historical context.

The second objective establishes long-term seafloor observatory sites by emplacing cased boreholes at summit (conduit) holes in three mud volcanoes (at Expedition 366 proposed Sites MAF-11A, MAF-9B, and MAF-15A) and removing the circulation obviation retrofit kit (CORK) body from Ocean Drilling Program Hole 1200C. These activities set the foundation for future deployments of sensors and samplers with the possibility of deploying a CORK-Lite structure within the boreholes. CORK-Lites provide a framework for conducting temporal observations that will allow one to “take the pulse of subduction” in an active nonaccretionary convergent plate margin and establish a platform for in situ experimentation.

Schedule for Expedition 366

International Ocean Discovery Program (IODP) Expedition 366 is based on IODP drilling Proposals 505-Full5 and APL-693 (available at **http://iodp.tamu.edu/scienceops/expeditions/mariana_convergent_margin.html**). Following ranking by the IODP Scientific Advisory Structure, the expedition was scheduled for the R/V *JOIDES Resolution*, operating under contract with the *JOIDES Resolution* Science Operator (JRSO). At the time of publication of this *Scientific Prospectus*, the expedition is scheduled to start in Guam on 8 December 2016 and to end in Hong Kong on 7 February 2017. A total of 56 days will be available for the transit, drilling, coring, and downhole measurements described in this report (for the current detailed schedule, see **http://iodp.tamu.edu/scienceops**). Further details about the facilities aboard the *JOIDES Resolution* can be found at **http://iodp.tamu.edu/labs/ship.html**.

The supporting site survey data for Expedition 366 are archived in the IODP Site Survey Data Bank (**http://ssdb.iodp.org/SSDBquery/SSDBquery.php** [select Proposal Number P505]).

Background and geological setting

Geologic processes at convergent plate margins control geochemical cycling, seismicity, and deep biosphere activity in subduction zones. Two approaches are typically taken to study such zones. One approach is to characterize inputs into a convergent plate margin by sampling the downgoing plate (e.g., Plank and Langmuir, 1993; Chan and Kastner, 2000). These inputs provide the geochemical reference necessary to elucidate what geochemical factors may influence the production of suprasubduction zone crust and mantle. A second approach is to study outputs in terms of magma and volatiles in volcanic arcs and backarc basin settings (e.g., Sano and Williams, 1996; Kelemen and Manning, 2015). Such outputs constrain processes that exist deep within the subduction zone. However, neither approach is able to constrain processes that occur within the large and dynamic zone that exists between the site where the subducting plate enters the trench and the location where it reaches the zone of magma genesis beneath the arc.

Determining unequivocally the composition of slab-derived fluids and their influences over the physical properties of the subduction zone or geochemical cycling in convergent margins requires direct sampling of the décollement region. Most studies of décollement materials, mass fluxes, and geochemical interchanges have been based on data from samples of drill cores, borehole observatories (circulation obviation retrofit kits [CORKs]), and mud volcanoes in accretionary convergent margins, as well as models based on geophysical considerations (e.g., Kastner et al., 1993; Carson and Westbrook, 1995; Maltman et al., 1997; Saffer et al., 2000; Hensen et al., 2004; Peacock et al., 2005; Solomon et al., 2009; Tryon et al., 2010). However, large wedges of accreted sediment bury the underlying crystalline basement, making it inaccessible by drilling, and the wedges interact with slab-derived fluids, altering the original slab chemical signal. Thus, dehydration reactions and metamorphic interchanges in intermediate and deeper parts of the décollements have yet to be sampled in these margins.

In contrast, nonaccretionary convergent margins can provide a more pristine slab-fluid signature because there is no thick accretionary sediment wedge for the fluids to interact with and fluid and material egress occurs through fault zones that have experienced water-rock interactions for millions of years, thus minimizing exchange during ascent (Fryer, 1996). Regardless of the type of margin, the deeper décollement region is directly inaccessible with current or even foreseeable ocean drilling technologies. Thus, a locality where a natural process brings materials from great depths directly to the surface will advance our knowledge of physical and chemical conditions along the décollement. The Mariana convergent margin provides precisely this type of environment (e.g., Fryer, 2012). Here, active serpentinite mud volcanoes provide a window to the décollement (Fryer and Fryer, 1987; Wheat et al., 2008) (Figure **F1**).

The Mariana subduction system is nonaccretionary and the forearc is pervasively faulted (Fryer, 1992). Here, serpentinite mud volcanoes are numerous, large (averaging 30 km diameter and 2 km high), and active (Fryer and Fryer, 1987; Fryer, 1992, 1996) (Figure **F2**). These mud volcanoes are composed principally of unconsolidated flows of serpentine muds containing clasts of serpentinized mantle peridotite and several other lithologies, including blueschist materials derived from the subducting slab (e.g., Maekawa et al., 1995; Fryer, 2012; Pabst et al., 2011), via deep-seated faults. Faulting within the forearc penetrates to great depths where fault gouge is produced and mobilized by slab-derived fluid, generating a thick gravitationally unstable slurry of mud and rock that rises to the seafloor within conduits along fault planes, particularly where faults intersect, producing large edifices over millions of years (Lockwood, 1972; Fryer, Pearce, Stokking, et al., 1990; Phipps and Ballotti, 1992; Fryer, 1996, 2012). Such fault intersections exist at a range of distances from the trench axis, which is a proxy for the depth to the subducting slab, allowing one to monitor the transformation of physical and geochemical processes as the lithosphere subducts (Figure F3).

Fluids upwell within these mud volcanoes at a rate that is in excess of the mud matrix (Fryer et al., 1999; Hulme et al., 2010). Such fluids originate from the downgoing plate but are highly altered, are reducing, and have pH values in the range of 9 to 12.5 (Mottl et al., 2003, 2004; Wheat et al., 2008; Hulme et al., 2010). Such fluids support distinct deep and shallow biospheres (Mottl et al., 2003; Takai et al., 2005; Curtis et al., 2013). The presence of microbial activity coupled with chemical products of the serpentinite formation spur the possibility that such systems have the potential to foster the origin of life on Earth (Bada and Lazcano, 2002; Schulte et al., 2006; Russell et al., 2010; Pons et al., 2011; Schrenk et al., 2013; Wang et al., 2014; Holm et al., 2015). Although currently the extent, activity, and evolution of this biosphere is unknown, the fundamental characterization of this community has been documented (Takai et al., 2005; Curtis et al., 2013). Furthermore, these microbial-laden upward-flowing fluids support megafaunal communities at seep sites (Fryer, 2012; Ohara et al., 2012).

In summary, mud volcanoes in the Mariana forearc are currently the most direct route to the décollement on Earth and because they exist at a range of distances from the trench, they provide a window that allows us to document processes and conditions at depths to ~20 km beneath the forearc (Oakley et al., 2007; Hulme et al., 2010) (Figure F2). Although the Mariana forearc represents the only current active serpentine mud volcanism in a convergent margin setting, such activity has occurred worldwide over the past 3.8 billion years (Pons et al., 2011) and maybe longer.

Motivation and scientific objectives

During the decade that Proposal 505-Full was under consideration for drilling, there have been significant advances in (1) our understanding of the Mariana forearc region and serpentinization processes in general, (2) the development of the field of subseafloor microbial research, (3) analytical capabilities, and (4) the capability and diversity of borehole sensors and samplers. Nevertheless, the main tenets of the proposal remain significant to our further understanding of convergent systems. Here, we revitalized the scientific motivation for Proposal 505-Full in the form of four interrelated research thrusts.

1. Mass transport processes in the Mariana forearc region

Fluid transport

Most of the fluid flow in the Mariana forearc is channeled along forearc faults and fault-controlled conduits in mud volcanoes (Fryer et al., 1999; Hulme et al., 2010). Such fluids ascend along mud-volcano conduits, likely traveling through well-established paths in contact with previously metamorphosed wall rock, preserving the fluid's slab signature. Other fluid paths may be less direct and slower, increasing the residence time that such fluids spend within the serpentinite matrix. Thus, one expects a range of pore fluid compositions depending on the nature of the channeling structures (diffuse network of small faults, major faults, and mud volcano conduits). A range of pore fluid compositions was recovered from the Conical Seamount, drilled during Ocean Drilling Program (ODP) Leg 125 (Fryer, Pearce, Stokking, et al., 1990) (Figures F2, F4). The summit site (ODP Site 780) produced the "purest" slab-derived fluids, based on the lower pore fluid chlorinity and higher concentrations of K, Rb, B, H_2S, and sulfate than the other sites. In contrast, the flank sites (ODP Sites 778 and 779) have pore fluids that are a combination of slab-derived fluid with seawater that had reacted with peridotite and basalt at shallower crustal depths (Mottl, 1992). The operational plan to core sites at the summits of the three mud volcanoes allows us to document variability of fluid transport and composition along strike of the southern forearc as the downgoing plate subducts and to core sites on the flanks of these mud volcanoes to evaluate temporal changes in pore fluids within distinct mudflow units that are and have been in a diffusion-reaction dominated environment for potentially millions of years.

Mechanics and rheology

The mechanics and rheology of serpentine muds in the Mariana forearc seamounts control processes that form the seamounts and their morphology (reviewed in Fryer, 2012). Coring three new seamounts will allow us to collect material from various mudflows and conduits within a range of morphologic surface features to place constraints on the mechanics that generate and emplace serpentinite muds, maintain the conduits, and construct seamounts.

Shipboard torsion-vane testing during Leg 125 at the Conical Seamount in the Mariana forearc and at the Torishima Forearc Seamount in the Izu-Bonin forearc showed that the serpentine muds are plastic solids (Fryer, Pearce, Stokking, et al., 1990). The rheology of these muds has many similarities to the idealized Cam clay soil model, which is well described by critical-state soil mechanics (Phipps and Ballotti, 1992). These muds are orders of magnitude weaker than salt and are, in fact, comparable in strength to common deep-sea pelagic clays. From analysis of flow morphology, based on bathymetry data, side-scan imagery, and remotely operated vehicle (ROV) observations, it is clear that there is considerable variability in volume and viscosity of individual flow units. This variability was highlighted during ODP Leg 195, during which the excellent recovery using advanced piston corer (APC)/extended core barrel (XCB) coring at ODP Site 1200 provided an opportunity to describe and sample a range of thin flows (Salisbury, Shinohara, Richter, et al., 2002). Critical to rheologic studies will be the analysis of the physical properties of muds from both the active summit regions and flank sites, including collection and preservation of whole-round samples for mechanical, stress, and permeability testing in shore-based laboratories.

Fluid budgets

Although total fluid budgets are difficult to ascertain in any convergent margin, the Mariana forearc provides easily discernable pathways for fluid expulsion related to hydrologic flow systems at accretionary margins. Furthermore, conduits that are dewatering the downgoing plate in the Mariana forearc persist for tens of millions of years, much longer than their accretionary counterparts. Attempts to determine the fluid budgets at accretionary active margins have been hindered by the presence of lateral heterogeneity and transient flow conditions that apparently result from the valve-like influence of accretionary complexes themselves.

Sediment properties in the underlying lithospheric plate differ with fluid pressure, and fluid pressure varies as a function of fluid production rate and transient hydrologic properties. Thus, an accretionary system acts as both a seal and a relief valve on the fluid flow system (Saffer et al., 2000). The absence of such a short timescale, fluid pressure, and a formation-properties modulator at nonaccretionary systems should allow fluids to escape more steadily. To test this hypothesis, the physical nature of fluid flow at nonaccretionary settings must be determined. Then fluid budgets can be constructed to determine whether the expected long-term flow is consistent with observations or if the flow must occur transiently. Expedition 366 will emplace casing within boreholes on each of the three summit drill targets, and postcruise emplacement of CORK-Lites (Wheat et al., 2012) at these sites, as well as one at the South Chamorro Seamount Hole 1200C, will establish along- and across-strike transects of seafloor observatory sites with which to address this and a range of other questions.

2. *Spatial variability of slab-related fluids*

Across-strike variability

The geochemistry of fluids from ODP cores and borehole fluids collected from Conical and South Chamorro Seamounts is described in detail in several publications (Fryer, Pearce, Stokking, et al., 1990; Haggerty, 1991; Haggerty and Chaudhuri, 1992; Haggerty and Fisher, 1992; Mottl, 1992; Mottl and Alt, 1992; Mottl et al., 2003, 2004; Hulme et al., 2010; Wheat et al., 2008, 2010). These investigators have shown the origin of the pore fluids results from dehydration of oceanic crustal basalt and sediment at the top of the subducting lithospheric slab. The compositions of the fluids from additional serpentinite mud volcanoes sampled by gravity and piston coring from surface ships also indicate a slab source and show progressive changes in the composition of pore fluids with distance from the trench correlate with hypothetical dehydration and decarbonation reactions that are expected to occur (Fryer et al., 1999; Mottl et al., 2004; Hulme et al., 2010).

Along-strike variability

Similarly, pore fluid data from drilling and piston coring from a number of seamounts suggest that the composition of slab-derived fluids and deep-derived rock materials may differ along the strike of the forearc, reflecting regional variations in composition within the slab and suprasubduction zone lithosphere. Such differences are probably associated not only with the depth to the slab but also with the physical conditions under which water-rock reactions occur and variations in the regional composition of the plate and overriding forearc wedge. In addition, microbial interaction with fluids, particularly in the shallow regions of the conduits, affects abundances of some constituents (Mottl et al., 2003; Takai et al., 2005; Curtis et al., 2013). Whether there are deeper effects and how microbial processes may vary over time is still unknown.

3. *Metamorphic and tectonic history and physical properties of the subduction zone*

Geochemical indicators from fluids

The composition of slab-derived and deep-derived metamorphosed rock is useful in defining geochemical processes and estimates of the thermal and pressure regime at depth and for determining physical properties of the décollement region. It is possible to constrain some of the pressure and temperature conditions under which certain dehydration reactions take place in the subducted slab (Peacock, 1996; Kincaid and Sacks, 1997; Mottl et al., 2003; Fryer et al., 2006). Pore fluids from Site 780 at the summit of Conical Seamount are unusual because of geochemical and physical processes at depth. The observed enrichments in alkali elements and B in fluids from Site 780 are unambiguous indicators of a source temperature in excess of 150°C (Shipboard Scientific Party, 1990b). The fact that these elements are depleted at Sites 778 and 779 on the flanks of the Conical Seamount, relative to their concentrations in seawater, indicates that the deep-slab signal can readily be overprinted by local peridotite-seawater reactions at lower temperatures. Not all chemical species are affected by this overprinting, however (i.e., sulfur isotopic composition of dissolved sulfate) (Mottl and Alt, 1992). Thus, to avoid potential reactions between sediment and slab-derived fluids and to study the most pristine slab-derived fluids possible, we need to collect fluids from mud volcano conduits where continued focused flow provides a pathway for slab-derived "basement" fluids to reach the seafloor. The locations of the summit sites on each seamount were chosen based on observed active springs. A small transect of holes at each summit site will permit us to determine the current location of the most focused fluid flow.

In order to study the effects of changes in composition of pore fluids within surficial mudflows with time and potential effects on underlying mudflows of burial by younger ones, we plan to core the flanks of the edifices. Flank sites were chosen at distal edges of mudflows in order to sample cores from the target flow and the immediately underlying flow(s). Additional holes drilled at each site, upflank and downflank from the target site, are planned to facilitate reaching this goal by examining contacts between overlapping mudflows. At the base of Big Blue Seamount, such an approach will also help to ascertain the effect of contact of the mudflows with underlying forearc sediments by coring through the base of the distal flank flows at Big Blue Seamount.

Metamorphic paragenesis

Studies of deep-derived minerals and metamorphic rock fragments brought to the surface in mudflows in these seamounts will permit us to constrain the pressure and temperature regimes under which metamorphism occurred (Fryer et al., 2006; Gharib, 2006). We know, for instance, that the minimum pressures of formation for incipient blueschist materials from Conical Seamount are 6–7 kbar (Maekawa et al., 1995). We estimate from the paragenesis of crossite schist recovered in cores from South Chamorro Seamount that pressures in excess of 7 kbar are consistent with their metamorphism (Fryer et al., 2006; Gharib, 2006). With stratigraphic control and deeper penetration (than that afforded by gravity and piston coring) of the muds from the three target edifices, we will be able to quantify the assemblages of rock clasts within the mudflows and constrain the ranges of pressure and temperature of the source regions of these materials. If age constraints from intercalated sediments are obtained, the temperature and pressure conditions of the décollement region through time would be better quantified.

Microtextural implications

The peridotite clasts enclosed in serpentinite cores recovered from prior ODP drilling, from gravity and piston coring, and peridotites recovered from dredge hauls or via ROVs or human-occupied vehicles are at least partially serpentinized. Extant olivine grains, however, are common in these rocks and can be used to identify different structural orientations of the peridotites. The crystal-preferred orientation (CPO) of olivine grains in the serpentinized rocks provides information on stress patterns within the forearc mantle wedge. One can detect horizontal extension, lateral shear, or upwelling that the crystals in a given rock have experienced, relative to the crystallographic directions of olivine grains (e.g., Michibayashi et al., 2007, 2012), and this can be related to anisotropy with accompanying serpentinization in the mantle (e.g., Katayama et al., 2009). Combining analysis of microtextures in the peridotites with rheological information from strain rate–dependent and temperature-dependent processes will provide a more detailed view of the history of variability along-strike of strain partitioning in the southern Mariana forearc mantle (e.g., Kneller and van Keken, 2007). Serpentine, particularly antigorite, has also been shown to develop strong acoustic anisotropy and CPO patterns that may contribute to regional variability in seismic anisotropy of the forearc mantle (e.g., Nishii et al., 2011). Detailed investigations of textures in the serpentinized peridotite clasts from the target sites will provide a historical context for the shallow- to intermediate-depth forearc mantle stress history. In addition, although rock clasts brought up from the subduction plate (metabasite schists) are only a minor component of the population of rocks recovered from the serpentinite mudflows, they do provide the constraints necessary to determine pressure and temperature conditions along the décollement. Furthermore, anisotropy implications for the subducting plate itself can be obtained from microtextural investigations of these slab-derived schists (Kim et al., 2013).

4. *Biological activity associated with deep-derived subduction zone material*

The interest in research pertaining to a deep subsurface biosphere has developed as a result of the study of extreme environments and their possible link to early Earth. Microbes and microbial products are abundant in oceanic hydrothermal environments and are presumed to be representative of a community of thermophilic and hyperthermophilic organisms that originate beneath the seafloor and potentially on extraterrestrial worlds (e.g., Fisk et al., 2000; Kelley et al., 2001; Reysenbach et al., 2006; Hellevang et al., 2011). Microbes are also involved in the transformation of minerals in the oceanic volcanic crust and in the cycling of elements within the crust; however, the ultimate origin of such microbes is controversial. In fact, investigators have suggested, for some time, that the first biomolecules would have preferred a cooler environment, as nucleic acids, critical to polymer stability, deteriorate rapidly at elevated temperatures (e.g., Lindhal, 1993; Bada and Lazcano, 2002). The investigation of sites with serpentinization point toward potential locations for life to evolve (e.g., Schulte et al., 2006; Russell et al., 2010; Schrenk et al., 2013; Lee et al., 2014; Holm et al., 2015) and serpentinite mud volcanism at convergent plate margins provides an excellent candidate locality (Pons et al., 2011; Fryer, 2012).

Drilling at both the active summit areas and the older flank mudflow lobes provides a unique opportunity to reexamine the hypothesis that microbes are capable of using alternative energy sources that would support either an autotrophic or a heterotrophic subsurface ecosystem and how that ecosystem might have changed with time. In addition, because pore fluids emanating from summit springs are more pristine in nonaccretionary convergent margins, it will be easier to assess from the chemistry of both the muds and the fluids whether inorganic synthesis is capable of supporting life.

Understanding the origin of the deep biosphere is fundamental to the IODP program and will further address the compelling question of whether life arose in these types of environments rather than in hydrothermal systems at oceanic spreading centers of the early Earth. Although a variety of studies indicate that a nonhyperthermophilic origin of life associated with serpentinization reactions is possible (e.g., Bada and Lazcano, 2002; Russell et al., 2010; Sleep et al., 2011; Valley et al., 2013; Holm et al., 2015), definitive proof will depend on how successful future efforts, such as studying the material from these active convergent margin sites, are at demonstrating that, at these conditions, organic components exist in the subsurface environment and on how such efforts are successful at learning how they respond to fluctuations in activity at such sites.

Drilling strategy

Previous drilling operations on Mariana serpentinite mud volcanoes

Two active serpentinite mud volcanoes have been drilled in the Mariana forearc region, the Conical Seamount during Leg 125 (Sites 778 and 779 on the flank and Site 780 on the summit) and the South Chamorro Seamount during Leg 195 (Site 1200) (Figures **F1**, **F4**, **F5**) (Shipboard Scientific Party, 1990c, 2002). Site 778 was initiated with a rotary core barrel (RCB) system and immediately encountered hole instability. Coring operations penetrated 107.6 m but only recovered 22.8 m of material (21% recovery) before it was abandoned. Site 789, another flank site, was drilled using RCB and penetrated 317.2 m but only recovered 73.2 m of material (23% recovery). Owing to the high risk to the drill string and logging tools, it was considered unsafe to log Hole 779A (Shipboard Scientific Party, 1990c). At the summit, Site 780 was drilled using RCB to a maximum penetration of 163.5 m in Hole 780C but only recovered 14.4 m of material (8.8% recovery). An attempt to log the hole failed because of hole instability.

Poor recovery and hole conditions set the set stage for changing drilling techniques during Leg 195. Site 1200 on the South Chamorro Seamount (Figure **F5**) was cored using APC operations. When hard clasts were encountered, an XCB center-bit assembly was deployed to drill through such clasts before returning to APC coring (Shipboard Scientific Party, 2002). Recovery of cored material using APC was ~100%. In addition to coring, a borehole observatory (CORK) was deployed in Hole 1200C with a screened section spanning 202.3 to 148.8 meters below seafloor (mbsf) (Davis et al., 1992; Shipboard Scientific Party, 2002). This original-style CORK persisted for several years before the data logger and internal package were recovered. Fluids now vent (~2 L/s) from the open orifice, providing access to pristine formation fluids at the seafloor (Wheat et al., 2008).

Expedition 366 operational strategy

Operations will occur on four serpentinite mud volcanoes and will start at the South Chamorro Seamount (Tables **T1**, **T2**). Here we will recover the original-style CORK body that was deployed during Leg 195 in Hole 1200C. Currently, formation fluids are discharging from the 4 inch annulus of the CORK body because a plug was removed in 2009 to allow sampling of fluids within the borehole. By removing the CORK body, we expand this opening to ~10 inches (25 cm) so that a CORK-Lite can be deployed, serving a range of scientific interests for future deployments of sensors and samplers within the borehole. Once the CORK body is removed, an ROV landing platform will be deployed. Operations in Hole 1200C result from Proposal APL-693; the rest of this expedition's operations are based on Proposal 505-Full5 (**http://iodp.tamu.edu/scienceops/expeditions/mariana_convergent_margin.html**).

Operations will then commence at the Blue Moon Seamount (proposed Sites MAF-15A and MAF-16A.) Coring operations will begin on the northwest flank of the seamount (Site MAF-16A) with two 50 m deep boreholes and one that is up to 250 m deep, forming a transect. Ideally these holes will intersect at least one complete flow event. Coring will begin with the APC system. If recovery of material is less than ideal we will switch to the half-length advanced piston coring (HLAPC) system. If recovery with the HLAPC system becomes less than ideal we will switch to the XCB system to advance the hole. There is no plan to use the RCB drilling system because of the disturbance it causes to recovered material from these serpentinite formations.

The same order of coring operations will occur at the summit site (MAF-15A); two 50 m deep boreholes and one up to 200 m deep will form a transect with the 200 m deep hole in the most active area of fluid upwelling that was determined during ROV operations in 2003. The transect of holes at this site and the other summit sites can lie within 500 m lateral distance of the site location in Table **T1**. Where the flow is most active, we will deploy a cased borehole with an ROV landing platform. This cased hole will consist of (from depth [~200 mbsf] to seafloor): a 10¾ inch casing shoe, one joint of 10¾ inch casing, a mechanical bridge plug, four joints of perforated and screened 10¾ inch casing, joints of 10¾ inch casing, a transition segment to 16 inch casing (casing swage), a 16 inch casing hanger, a reentry cone assembly, and an ROV platform. This cased hole will be deployed with a mud motor, underreamer, and drill bit. Once completed, we may attempt to collect a water sample within the borehole. Given that these mud volcanoes are permeable and overpressured, they should vent formation fluids (e.g., as at the South Chamorro Seamount). Once completed, the borehole will be ready for a future deployment of a CORK-Lite (Wheat et al., 2012). Should problems arise while drilling-in the casing, hardware will be present so that we can complete the borehole deployment as was done for the casing in Hole 1200C.

Next, we will transit to the Big Blue Seamount. Similar to the Blue Moon Seamount, we will core the flank sites first (proposed Sites MAF-14A, MAF-13A, and MAF-12B), each with two 50 m deep boreholes and one 250 m deep borehole. Here the goal is to penetrate a (or multiple) complete serpentinite mudflow(s). In the case of Site MAF-14A, we plan to penetrate to 350 mbsf through the entire serpentinite flow into the regional "normal" sedimented crust. The summit will be cored (proposed Site MAF-11A) with two 50 m deep holes and one 200 m deep hole. The cased borehole with ROV landing platform will be located in the most active site of fluid flow as determined during the 2003 ROV operations. This cased borehole will be identical to the one deployed at the Blue Moon Seamount.

We will start operations at the fourth and final seamount with coring at the summit of the Celestial Seamount (proposed Site MAF-9B). Two 50 m deep holes and one 200 m deep hole will form a transect toward the most active site of fluid flow, as determined during 2003 ROV operations. Here, we will deploy a cased borehole identical to the ones at the Big Blue and Blue Moon Seamounts. Following operations at the summit we will descend the flanks and drill proposed Site MAF-10B. Here, two 50 m deep holes and one 300 m deep hole will be placed to penetrate a complete serpentinite flow and penetrate into the regional sedimented crust below.

Downhole measurements strategy

Formation temperature and pressure measurements

We plan to use the advanced piston corer temperature tool (APCT-3) to measure formation temperature deeper than 20 mbsf (preferably starting with the third core of each hole) and continue with depth as drilling constraints allow. We also will use the sediment temperature/pressure (SETP) tool and/or the temperature dual-pressure (T2P) probe, if available, to measure in situ pressure. Such measurements are especially desired within the summit (conduit) region of each of the three seamounts that will be cored.

Downhole wireline logging

Given the well-documented tendency of the serpentinite matrix to collapse, resulting in hole instabilities, and the short (<300 m) boreholes, there is no plan to log any of the summit sites. However, some of the flank sites are positioned with the intention of penetrating the underlying regional forearc sediment. Such holes may offer the opportunity to log the transition from serpentinite to "normal" underlying oceanic sediment sequences. Should such a situation arise, we would use the triple combo and the Formation MicroScanner (FMS)-sonic tool strings. However, safety and coring are top priorities at each site, so wireline logging is unlikely.

Contingencies

There are three distinct operations that will be conducted during Expedition 366. First, we will remove the CORK body from Hole 1200C. If the CORK body is not removed in 8 h after mating with the CORK body, then we will unlatch from the CORK body, recover the drill string and proceed to the Blue Moon Seamount. Currently, the borehole is open to seawater and discharging formation fluid.

The second operational activity is coring. Serpentinite muds are very "sticky" and may bind the drill pipe. Should we have issues in a particular hole, we will pull out of the hole, offset, and try again. Should these issues continue into the next hole, we will keep nonrotational operations to a minimum and try to reach the desired depth. At the flank sites where we plan to reach sedimented crust below the serpentinite flows, we have the option to move 1 km downslope where the sedimented crust can be accessed more easily at a shallower depth below seafloor.

Lastly, another distinct operation is the deployment of cased boreholes. The plan is to drill the boreholes in place. Should issues arise during deployment, we have the option to use a standard casing deployment (e.g., similar to operations that resulted in the cased borehole in Hole 1200C). Such a deployment would start by jetting in two joints of 20 inch casing or four joints of 16 inch casing, both including a hanger. For the case involving the 20 inch casing, a second pipe trip would lower and drill in about 100 m of 16 inch casing with a casing hanger. In either case (starting with 20 or 16 inch casing) the hole would be drilled to depth and cleaned out repeatedly. Heavy mud could be left in the borehole while the 10¾ inch casing string is assembled and lowered into place.

If we are efficient and operate faster than anticipated, we can add additional holes to extend transect length at various sites.

Risks

Several potential risks were examined, and are considered to be of low likelihood of affecting the success of the expedition, based on the following rationales.

Environmental issues

The summit region of these serpentinite mud volcanoes is a unique environment in the world's oceans, and benthic communities at the summit of seamounts could be affected by drilling activity. Considering the four sites that will be visited during Expedition 366, the only active benthic community is at the South Chamorro Seamount. A return with the *Jason-2* ROV to the South Chamorro Seamount 2 y after drilling during Leg 125 revealed a benthic community that was still thriving.

Potential gas traps

Methane content in the serpentinite muds from these volcanoes is a product of methanogenic microbial activity (Curtis et al., 2013). No bottom-simulating reflectors are evident on the multichannel seismic (MCS) data from surveys of these mud volcanoes. In addition, the internal structure of each of the edifices is heterogeneous and shows no potential hydrocarbon trapping structures and there is known venting. The largest concentration of methane that was measured in samples from the Conical Seamount (32 mmol/kg) was from a short (one core) interval. We conclude that any methane present will not cause any problems.

Currents and physical obstructions

There are no strong currents in the region, as determined by numerous operations during previous cruises. There are no seafloor cables in the regions that are targeted for this expedition.

Weather (El Niño 2015–2016)

The higher incidence of tropical storms that currently exists in the Pacific is expected to return to normal toward the end of 2016. The typical weather pattern for the area around Guam is generally favorable with regard to a low incidence of typhoons, but the current schedule places the ship within the windy season for this area. Thus, sea states may be somewhat of a challenge.

Logistical challenges

The only logistical challenge for this expedition is that operations at Site 1200, related to APL-693, will require clearance from the US Navy regarding deconflicting with any potential Naval exercises in the area.

Sampling plan

Shipboard and shore-based researchers should refer to the IODP Sample, Data, and Obligations Policy and Implementation Guidelines (**http://www.iodp.org/doc_download/4038-iodp-sample-data-and-obligations-policy**). This document outlines the policy for distributing IODP samples and data to research scientists, curators, and educators. The document also defines the obligations that sample and data recipients incur. The Sample Allocation Committee (SAC) will work with the entire scientific party to formulate a formal expedition-specific sampling plan for shipboard and postcruise sampling. The SAC is composed of the Co-Chief Scientists, Expedition Project Manager (EPM), and IODP Curator on shore and curatorial representative in place of the Curator on board the ship.

We expect to recover a total of 2000–3000 m of serpentine mudflows containing an assortment of rock clasts of various lithologies (about 5%–10% by volume) and ~150 m of pelagic sediment. We will also retrieve an original-style CORK body from Hole 1200C. The volume and frequency of samples taken from the working half of the cores must be justified on the basis of scientific merit and will depend on core recovery, the full spectrum of other requests, and expedition objectives.

Every member of the science party is obligated to conduct scientific research for the expedition and publish results. Shipboard and shore-based scientists are expected to submit sample requests (at **http://web.iodp.tamu.edu/sdrm**). Sample requests to be considered as highest priority need to be received by 1 June 2016 (6 months before departure). Such timing is necessary to accommodate a vast whole-round and discrete sampling program so that the appropriate freezers and supplies can be sent to the ship to meet the demand created through sample requests. We anticipate that certain shipboard and shore-based participants may require specific sampling methods. Participants are encouraged to identify any specific needs in their requests. Some redundancy of measurements is unavoidable, but minimizing replication of measurements between the shipboard party and identified shore-based collaborators will be a factor in evaluating sample requests. The sampling plan will be subject to modification depending on the actual material recovered and collaborations may evolve between scientists during the expedition. Modifications of any sampling plan during the expedition must be approved by the Co-Chief Scientists, EPM, and curatorial representative.

If some critical intervals are recovered (e.g., fault gouge, ash layers, basement veins, or serpentinite/pelagic interface), there may be considerable demand for samples from a limited amount of cored material. These intervals may require special handling that may affect sample density and size and minimize continuous (whole-round) core sampling by a single investigator. A sampling plan coordinated by the SAC may be required before critical intervals are sampled.

All collected data and samples will be protected by a 1 y postexpedition moratorium, during which time data and samples are available only to the Expedition 366 shipboard science party and approved shore-based participants. This moratorium will begin once the shipboard science party disembarks.

Expedition scientists and scientific participants

The current list of participants for Expedition 366 can be found at **http://iodp.tamu.edu/scienceops/expeditions/mariana_convergent_margin.html**.

References

Bada, J.L., and Lazcano, A., 2002. Some like it hot, but not the first biomolecules. *Science,* 296(5575):1982–1983.
http://dx.doi.org/10.1126/science.1069487

Carson, B., and Westbrook, G.K., 1995. Modern fluid flow in the Cascadia accretionary wedge: a synthesis. *In* Carson, B., Westbrook, G.K., Musgrave, R.J., and Suess, E. (Eds.), *Proceedings of the Ocean Drilling Program, Scientific Results,* 146 (Part 1): College Station, TX (Ocean Drilling Program), 413–421.
http://dx.doi.org/10.2973/odp.proc.sr.146-1.240.1995

Chan, L.-H., and Kastner, M., 2000. Lithium isotopic compositions of pore fluids and sediments in the Costa Rica subduction zone: implications for fluid processes and sediment contribution to the arc volcanoes. *Earth and Planetary Science Letters,* 183(1–2):275–290.
http://dx.doi.org/10.1016/S0012-821X(00)00275-2

Curtis, A.C., Wheat, C.G., Fryer, P., and Moyer, C.L., 2013. Mariana forearc serpentinite mud volcanoes harbor novel communities of extremophilic Archaea. *Geomicrobiology Journal,* 30(5):430–441.
http://dx.doi.org/10.1080/01490451.2012.705226

Davis, E.E., Becker, K., Pettigrew, T., Carson, B., and MacDonald, R., 1992. CORK: a hydrologic seal and downhole observatory for deep-ocean boreholes. *In* Davis, E.E., Mottl, M.J., Fisher, A.T., et al., *Proceedings of the Ocean Drilling Program, Initial Reports,* 139: College Station, TX (Ocean Drilling Program), 43–53.
http://dx.doi.org/10.2973/odp.proc.ir.139.103.1992

Fisk, M.R., Thorseth, I.H., Urbach, E., and Giovannoni, S.J., 2000. Investigation of microorganisms and DNA from subsurface thermal water and rock from the east flank of Juan de Fuca Ridge. *In* Fisher, A., Davis, E.E., and Escutia, C. (Eds.), *Proceedings of the Ocean Drilling Program, Scientific Results,* 168: College Station, TX (Ocean Drilling Program), 167–174. **http://dx.doi.org/10.2973/odp.proc.sr.168.022.2000**

Fryer, P., 1992. A synthesis of Leg 125 drilling of serpentine seamounts on the Mariana and Izu-Bonin forearcs. *In* Fryer, P., Pearce, J.A., Stokking, L.B., et al., *Proceedings of the Ocean Drilling Program, Scientific Results,* 125: College Station, TX (Ocean Drilling Program), 593–614. **http://dx.doi.org/10.2973/odp.proc.sr.125.168.1992**

Fryer, P., 1996. Evolution of the Mariana convergent plate margin system. *Reviews of Geophysics,* 34(1):89–125. **http://dx.doi.org/10.1029/95RG03476**

Fryer, P., 2012. Serpentinite mud volcanism: observations, processes, and implications. *Annual Review of Marine Science,* 4(1):345–373. **http://dx.doi.org/10.1146/annurev-marine-120710-100922**

Fryer, P., and Fryer, G.J., 1987. Origins of nonvolcanic seamounts in a forearc environment. *In* Keating, B.H., Fryer, P., Batiza, R., and Boehlert, G.W. (Eds.), *Seamounts, Islands, and Atolls.* Geophysical Monograph, 43:61–69. **http://dx.doi.org/10.1029/GM043p0061**

Fryer, P., Gharib, J., Ross, K., Savov, I., and Mottl, M.J., 2006. Variability in serpentinite mudflow mechanisms and sources: ODP drilling results on Mariana forearc seamounts. *Geochemistry, Geophysics, Geosystems,* 7(8):Q08014. **http://dx.doi.org/10.1029/2005GC001201**

Fryer, P., Pearce, J.A., Stokking, L.B., et al., 1990. *Proceedings of the Ocean Drilling Program, Initial Reports,* 125: College Station, TX (Ocean Drilling Program). **http://dx.doi.org/10.2973/odp.proc.ir.125.1990**

Fryer, P., Wheat, C.G., and Mottl, M.J., 1999. Mariana blueschist mud volcanism: implications for conditions within the subduction zone. *Geology,* 27(2):103–106. **http://dx.doi.org/10.1130/0091-7613(1999)027<0103:MBMVIF>2.3.CO;2**

Gharib, J., 2006. Clastic metabasites and authigenic minerals within serpentinite protrusions from the Mariana forearc: implications for subforearc subduction processes [Ph.D. dissertation]. University of Hawaii.

Haggerty, J.A., 1991. Evidence from fluid seeps atop serpentine seamounts in the Mariana forearc: clues for emplacement of the seamounts and their relationship to forearc tectonics. *Marine Geology,* 102(1–4):293–309. **http://dx.doi.org/10.1016/0025-3227(91)90013-T**

Haggerty, J.A., and Chaudhuri, S., 1992. Strontium isotopic composition of the interstitial waters from Leg 125: Mariana and Bonin forearcs. *In* Fryer, P., Pearce, J.A., Stokking, L.B., et al., *Proceedings of the Ocean Drilling Program, Scientific Results,* 125: College Station, TX (Ocean Drilling Program), 397–400. **http://dx.doi.org/10.2973/odp.proc.sr.125.124.1992**

Haggerty, J.A., and Fisher, J.B., 1992. Short-chain organic acids in interstitial waters from Mariana and Bonin forearc serpentines: Leg 125. *In* Fryer, P., Pearce, J.A., Stokking, L.B., et al., *Proceedings of the Ocean Drilling Program, Scientific Results,* 125: College Station, TX (Ocean Drilling Program), 387–395. **http://dx.doi.org/10.2973/odp.proc.sr.125.125.1992**

Hellevang, H., Huang, S., Thorseth, I.H., 2011. The potential for low-temperature abiotic hydrogen generation and a hydrogen-driven deep biosphere. *In* Cockell, C.S., Cady, S.L, and McLoughlin, N. (Eds.), *Volcanism and Astrobiology: Life on Earth and Beyond.* Astrobiology, 11(7):711–724. **http://dx.doi.org/10.1089/ast.2010.0559**

Hensen, C., Wallmann, K., Schmidt, M., Ranero, C.R., and Suess, E., 2004. Fluid expulsion related to mud extrusion off Costa Rica—a window to the subducting slab. *Geology,* 32(3):201–204. **http://dx.doi.org/10.1130/G20119.1**

Holm, N.G., Oze, C., Mousis, O., Waite, J.H., and Guilbert-Lepoutre, A., 2015. Serpentinization and the formation of H_2 and CH_4 on celestial bodies (planets, moons, comets). *Astrobiology,* 15(7):587–600. **http://dx.doi.org/10.1089/ast.2014.1188**

Hulme, S.M., Wheat, C.G., Fryer, P., and Mottl, M.J., 2010. Pore water chemistry of the Mariana serpentinite mud volcanoes: a window to the seismogenic zone. *Geochemistry, Geophysics, Geosystems,* 11(1):Q01X09. **http://dx.doi.org/10.1029/2009GC002674**

Kastner, M., Elderfield, H., Jenkins, W.J., Gieskes, J.M., and Gamo, T., 1993. Geochemical and isotopic evidence for fluid flow in the western Nankai subduction zone, Japan. *In* Hill, I.A., Taira, A., Firth, J.V., et al., *Proceedings of the Ocean Drilling Program, Scientific Results,* 131: College Station, TX (Ocean Drilling Program), 397–413. **http://dx.doi.org/10.2973/odp.proc.sr.131.143.1993**

Katayama, I., Hirauchi, K., Michibayashi, K., and Ando, J., 2009. Trench-parallel anisotropy produced by serpentine deformation in the hydrated mantle wedge. *Nature,* 461(7267):1114–1117. **http://dx.doi.org/10.1038/nature08513**

Kelemen, P.B., and Manning, C.E., 2015. Reevaluating carbon fluxes in subduction zones, what goes down, mostly comes up. *Proceedings of the National Academy of Sciences of the United States of America,* 112(30):E3997–E4006. **http://dx.doi.org/10.1073/pnas.1507889112**

Kelley, D.S., Karson, J.A., Blackman, D.K., Früh-Green, G.L., Butterfield, D.A., Lilley, M.D., Olson, E.J., Schrenk, M.O., Roe, K.K., Lebon, G.T., Rivizzigno, P., and the AT3-60 Shipboard Party, 2001. An off-axis hydrothermal vent field near the Mid-Atlantic Ridge at 30°N. *Nature,* 412(6843):145–149. **http://dx.doi.org/10.1038/35084000**

Kim, D., Katayama, I., Michibayashi, K., and Tsujimori, T., 2013. Deformation fabrics of natural blueschists and implications for seismic anisotropy in subducting oceanic crust. *Physics of the Earth and Planetary Interiors,* 222:8–21. **http://dx.doi.org/10.1016/j.pepi.2013.06.011**

Kincaid, C., and Sacks, I.S., 1997. Thermal and dynamical evolution of the upper mantle in subduction zones. *Journal of Geophysical Research: Solid Earth,* 102(B6):12295–12315. **http://dx.doi.org/10.1029/96JB03553**

Kneller, E.A., and van Keken, P.E., 2007. Trench-parallel flow and seismic anisotropy in the Mariana and Andean subduction systems. *Nature,* 450(7173):1220–1227. **http://dx.doi.org/10.1038/nature06429**

Lee, N., Foustoukos, D.I., Sverjensky, D.A., Cody, G.D., and Hazen, R.M., 2014. The effects of temperature, pH and redox state on the stability of glutamic acid in hydrothermal fluids. *Geochimica et Cosmochimica Acta,* 135:66–86. **http://dx.doi.org/10.1016/j.gca.2014.02.043**

Lindhal, T., 1993. Instability and decay of the primary structure of DNA. *Nature,* 362(6422):709–715. **http://dx.doi.org/10.1038/362709a0**

Lockwood, J.P., 1972. Possible mechanisms for the emplacement of alpine-type serpentinite. *Memoir - Geological Society of America,* 132:273–288. **http://dx.doi.org/10.1130/MEM132-p273**

Maekawa, H., Fryer, P., and Ozaki, A., 1995. Incipient blueschist-facies metamorphism in the active subduction zone beneath the Mariana forearc. *In* Taylor, B., and Natland, J. (Eds.), *Active Margins and Marginal Basins of the Western Pacific.* Geophysical Monograph, 88:281–290. **http://dx.doi.org/10.1029/GM088p0281**

Maltman, A., Labaume, P., and Housen, B., 1997. Structural geology of the décollement at the toe of the Barbados accretionary prism. *In* Shipley, T.H., Ogawa, Y., Blum, P., and Bahr, J.M. (Eds.), *Proceedings of the Ocean Drilling Program, Scientific Results,* 156: College Station, TX (Ocean Drilling Program), 279–292. **http://dx.doi.org/10.2973/odp.proc.sr.156.037.1997**

Michibayashi, K., Kasufuka, Y., Satsukawa, T., and Nasir, S.J., 2012. Seismic properties of peridotite xenoliths as a clue to imaging the lithospheric mantle beneath NE Tasmania, Australia. *Tectonophysics,* 522–523:218–223. **http://dx.doi.org/10.1016/j.tecto.2011.12.002**

Michibayashi, K., Tasaka, M., Ohara, Y., Ishii, T., Okamoto, A., and Fryer, P., 2007. Variable microstructure of peridotite samples from the southern Mariana Trench: evidence of a complex tectonic evolution. *Tectonophysics,* 444 (1–4):111–118. **http://dx.doi.org/10.1016/j.tecto.2007.08.010**

Mottl, M.J., 1992. Pore waters from serpentinite seamounts in the Mariana and Izu-Bonin forearcs, Leg 125: evidence for volatiles from the subducting slab. *In* Fryer, P., Pearce, J.A., Stokking, L.B., et al., *Proceedings of the Ocean Drilling Program, Scientific Results,* 125: College Station, TX (Ocean Drilling Program), 373–385. **http://dx.doi.org/10.2973/odp.proc.sr.125.121.1992**

Mottl, M.J., and Alt, J.C., 1992. Data report: minor and trace element and sulfur isotopic composition of pore waters from Sites 778 through 786. *In* Fryer, P., Pearce, J.A., Stokking, L.B., et al., *Proceedings of the Ocean Drilling Program, Scientific Results,* 125: College Station, TX (Ocean Drilling Program), 683–688. **http://dx.doi.org/10.2973/odp.proc.sr.125.184.1992**

Mottl, M.J., Komor, S.C., Fryer, P., and Moyer, C.L., 2003. Deep-slab fluids fuel extremophilic Archaea on a Mariana forearc serpentinite mud volcano:

Ocean Drilling Program Leg 195. *Geochemistry, Geophysics, Geosystems,* 4:9009. **http://dx.doi.org/10.1029/2003GC000588**

Mottl, M.J., Wheat, C.G., Fryer, P., Gharib, J., and Martin, J.B., 2004. Chemistry of springs across the Mariana forearc shows progressive devolatilization of the subducting plate. *Geochimica et Cosmochimica Acta,* 68(23):4915–4933. **http://dx.doi.org/10.1016/j.gca.2004.05.037**

Nakanishi, M., Tamaki, K., and Kobayashi, K., 1992. Magnetic anomaly lineations from Late Jurassic to Early Cretaceous in the west-central Pacific Ocean. *Geophysical Journal International,* 109(3):701–719. **http://dx.doi.org/10.1111/j.1365-246X.1992.tb00126.x**

Nishii, A., Wallis, S.R., Mizukami, T., and Michibayashi, K., 2011. Subduction related antigorite CPO patterns from forearc mantle in the Sanbagawa belt, southwest Japan. *Journal of Structural Geology,* 33(10):1436–1445. **http://dx.doi.org/10.1016/j.jsg.2011.08.006**

Oakley, A., 2008. A multi-channel seismic and bathymeric investigation of the central Mariana convergent margin [Ph.D. dissertation]. University of Hawaii. **http://www.soest.hawaii.edu/GG/resources/theses/Oakley Dissertation 2008.pdf**

Oakley, A.J., Taylor, B., Fryer, P., Moore, G.F., Goodliffe, A.M., and Morgan, J.K., 2007. Emplacement, growth, and gravitational deformation of serpentinite seamounts on the Mariana forearc. *Geophysical Journal International,* 170(2):615–634. **http://dx.doi.org/10.1111/j.1365-246X.2007.03451.x**

Ohara, Y., Reagan, M.K., Fujikura, K., Watanabe, H., Michibayashi, K., Ishii, T., Stern, R.J., Pujana, I., Martinez, F., Girard, G., Ribeiro, J., Brounce, M., Komori, N., and Kino, M., 2012. A serpentinite-hosted ecosystem in the southern Mariana forearc. *Proceedings of the National Academy of Sciences of the United States of America,* 109(8): 2831–2835. **http://dx.doi.org/10.1073/pnas.1112005109**

Pabst, S., Zack, T., Savov, I.P., Ludwig, T., Rost, D., Tonarini, S., and Vicenzi, E.P., 2011. The fate of oceanic slabs in the shallow mantle: insights from boron isotopes and light element composition of metasomatized blueschists from the Mariana forearc. *Lithos,* 132:162–179. **http://dx.doi.org/10.1016/j.lithos.2011.11.010**

Peacock, S.M., 1996. Thermal and petrologic structure of subduction zones. *In* Bebout, G.E., Scholl, D.W., Kirby, S.H., and Platt, J.P. (Eds.), *Subduction Top to Bottom.* Geophysical Monograph, 96:119–133. **http://dx.doi.org/10.1029/GM096p0119**

Peacock, S.M., van Keken, P.E., Holloway, S.D., Hacker, B.R., Abers, G.A., and Fergason, R.L., 2005. Thermal structure of the Costa Rica–Nicaragua subduction zone. *Physics of the Earth and Planetary Interiors,* 149(1–2):187–200. **http://dx.doi.org/10.1016/j.pepi.2004.08.030**

Phipps, S.P., and Ballotti, D., 1992. Rheology of serpentinite muds in the Mariana-Izu-Bonin forearc. *In* Fryer, P., Pearce, J.A., Stokking, L.B., et al., *Proceedings of the Ocean Drilling Program, Scientific Results,* 125: College Station, TX (Ocean Drilling Program), 363–372. **http://dx.doi.org/10.2973/odp.proc.sr.125.154.1992**

Plank, T., and Langmuir, C.H., 1993. Tracing trace elements from sediment input to volcanic output at subduction zones. *Nature,* 362(6422):739–743. **http://dx.doi.org/10.1038/362739a0**

Pons, M.-L., Quitté, G., Fujii, T., Rosing, M.T., Reynard, B., Moynier, F., Douchet, C., and Albarède, F., 2011. Early Archean serpentine mud volcanoes at Isua, Greenland, as a niche for early life. *Proceedings of the National Academy of Sciences of the United States of America,* 108(43):17639–17643. **http://dx.doi.org/10.1073/pnas.1108061108**

Reysenbach, A.-L., Liu, Y., Banta, A.B., Beveridge, T.J., Kirshtein, J.D., Schouten, S., Tivey, M.K., Von Damm, K.L., and Voytek, M.A., 2006. A ubiquitous thermoacidophilic archaeon from deep-sea hydrothermal vents. *Nature,* 442(7101)444–447. **http://dx.doi.org/10.1038/nature04921**

Russell, M.J., Hall, A.J., and Martin, W., 2010. Serpentinization as a source of energy at the origin of life. *Geobiology,* 8(5):355–371. **http://dx.doi.org/10.1111/j.1472-4669.2010.00249.x**

Saffer, D.M., Silver, E.A., Fisher, A.T., Tobin, H., and Moran, K., 2000. Inferred pore pressures at the Costa Rica subduction zone: implications for dewatering processes. *Earth and Planetary Science Letters,* 177(3–4):193–207. **http://dx.doi.org/10.1016/S0012-821X(00)00048-0**

Salisbury, M.H., Shinohara, M., Richter, C., et al., 2002. *Proceedings of the Ocean Drilling Program, Initial Reports,* 195: College Station, TX (Ocean Drilling Program). **http://dx.doi.org/10.2973/odp.proc.ir.195.2002**

Sano, Y., and Williams, S.N., 1996. Fluxes of mantle and subducted carbon along convergent plate boundaries. *Geophysical Research Letters,* 23(20):2749–2752. **http://dx.doi.org/10.1029/96GL02260**

Schrenk, M.O., Brazelton, W.J., and Lang, S.Q., 2013. Serpentinization, carbon, and deep life. *In* Hazen, R.M., Jones, A.P., and Baross, J.A. (Eds.), *Carbon in Earth.* Reviews in Mineralogy and Geochemistry, 75(1):575–606. **http://dx.doi.org/10.2138/rmg.2013.75.18**

Schulte, M., Blake, D., Hoehler, T., and McCollom, T., 2006. Serpentinization and its implications for life on the early Earth and Mars. *Astrobiology,* 6(2):364–376. **http://dx.doi.org/10.1089/ast.2006.6.364**

Shipboard Scientific Party, 1990b. Site 780. *In* Fryer, P., Pearce, J.A., Stokking, L.B., et al., *Proceedings of the Ocean Drilling Program, Initial Reports,* 125: College Station, TX (Ocean Drilling Program), 147–178. **http://dx.doi.org/:10.2973/odp.proc.ir.125.108.1990**

Shipboard Scientific Party, 1990c. Summary of results from Leg 125. *In* Fryer, P., Pearce, J.A., Stokking, L.B., et al., *Proceedings of the Ocean Drilling Program, Initial Reports,* 125: College Station, TX (Ocean Drilling Program), 367–380. **http://dx.doi.org/:10.2973/odp.proc.ir.125.115.1990**

Shipboard Scientific Party, 2002. Leg 195 summary. *In* Salisbury, M.H., Shinohara, M., Richter, C., et al., *Proceedings of the Ocean Drilling Program, Initial Reports,* 195: College Station, TX (Ocean Drilling Program), 1–63. **http://dx.doi.org/10.2973/odp.proc.ir.195.101.2002**

Sleep, N.H., Bird, D.K., and Pope, E.C., 2011. Serpentinite and the dawn of life. *Philosophical Transactions of the Royal Society, B: Biological Sciences,* 366(1580):2857–2869. **http://dx.doi.org/10.1098/rstb.2011.0129**

Solomon, E.A., Kastner, M., Wheat, C.G., Jannasch, H., Robertson, G., Davis, E.E., and Morris, J.D., 2009. Long-term hydrogeochemical records in the oceanic basement and forearc prism at the Costa Rica subduction zone. *Earth and Planetary Science Letters,* 282(1–4):240–251. **http://dx.doi.org/10.1016/j.epsl.2009.03.022**

Takai, K., Moyer, C.L., Miyazaki, M., Nogi, Y., Hirayama, H., Nealson, K.H., and Horikoshi, K., 2005. *Marinobacter alkaliphilus* sp. nov., a novel alkaliphilic bacterium isolated from subseafloor alkaline serpentine mud from Ocean Drilling Program Site 1200 at South Chamorro Seamount, Mariana forearc. *Extremophiles,* 9(1):17–27. **http://dx.doi.org/10.1007/s00792-004-0416-1**

Tryon, M.D., Wheat, C.G., and Hilton, D.R., 2010. Fluid sources and pathways of the Costa Rica erosional convergent margin. *Geochemistry, Geophysics, Geosystems,* 11(4):Q04S22. **http://dx.doi.org/10.1029/2009GC002818**

Valley, J.W., Peck, W.H., King, E.M., and Wilde, S.A., 2013. A cool early Earth. *Geology,* 30(4):351–354. **http://dx.doi.org/10.1130/0091-7613(2002)030<0351:ACEE>2.0.CO;2**

Wang, X., Ouyang, Z., Zhuo, S., Zhang, M., Zheng, G., and Wang, Y., 2014. Serpentinization, abiogenic organic compounds, and deep life. *Science China Earth Sciences,* 57(5):878–887. **http://dx.doi.org/10.1007/s11430-014-4821-8**

Wheat, C.G., Edwards, K.J., Pettigrew, T., Jannasch, H.W., Becker, K., Davis, E.E., Villinger, H., and Bach, W., 2012. CORK-lite: bringing legacy boreholes back to life. *Scientific Drilling,* 14:39–43. **http://dx.doi.org/10.2204/iodp.sd.14.05.2012**

Wheat, C.G., Fryer, P., Fisher, A.T., Hulme, S., Jannasch, H., Mottl, M.J., and Becker, K., 2008. Borehole observations of fluid flow from South Chamorro Seamount, an active serpentinite mud volcano in the Mariana forearc. *Earth and Planetary Science Letters,* 267(3–4):401–409. **http://dx.doi.org/10.1016/j.epsl.2007.11.057**

Wheat, C.G., Fryer, P., Takai, K., and Hulme, S., 2010. Spotlight 9: South Chamorro Seamount, 13°7.00′N, 146°00.00′E. *Oceanography*, 23(1):174–175. **http://www.tos.org/oceanography/issues/issue_archive/issue_pdfs/23_1/23-1_wheat.pdf**

Table T1. Expedition 366 sites. South Chamorro Seamount will not be drilled during Expedition 366; the existing hole is 140 m deep. NA = not applicable.

Site type	Site	Latitude	Longitude	Water depth (m)	Depth of penetration (mbsf)
South Chamorro Seamount					
Summit	1200C	13°47.07′N	146°0.17′E	2932	NA
Blue Moon Seamount					
Flank	MAF-16A	15°47.12′N	147°08.49′E	4500	250
Summit	MAF-15A	15°42.57′N	147°10.6′E	3666	200
Big Blue Seamount					
Flank	MAF-14A	17°59.53′N	147°06′E	3300	350
Flank	MAF-13A	18°03.09′N	147°06′E	2200	250
Flank	MAF-12B	18°05.67′N	147°06′E	1400	250
Summit	MAF-11A	18°06.4′N	147°05.9′E	1260	200
Celestial Seamount					
Summit	MAF-9B	16°32.25′N	147°13.25′E	2000	200
Flank	MAF-10B	16°27.6′N	147°10.35′E	3200	300

Table T2. Operations plan for primary proposed sites, Expedition 366. CORK = circulation obviation retrofit kit. EPSP = Environmental Protection and Safety Panel. APC = advanced piston corer, XCB = extended core barrel.

Site	Location (Latitude Longitude)	Seafloor depth (mbrf)	Operations description	Transit (days)	Drilling coring (days)
Guam			Begin expedition 5.0	Port call days	
			Transit ~0 nmi to WP-01 @ 10.5 kt, ~0 nmi to WP-02 @ 2.0 kt, ~2 nmi to WP-03 @ 2.0 kt, and ~1 nmi to WP-04 @ 2.0 kt, ~24 nmi to WP-05 @ 10.5 kt, and ~67 nmi to MAF-4B (Hole 1200C CORK recovery) @ 10.5 kt	0.4	
MAF-4B (1200C CORK recovery)	13°47.07'N	2943	Hole 1200C - re-CORK	0.0	3.3
EPSP to 0 mbsf	146°0.17'E				
			Subtotal days on-site: 3.3		
			Transit ~137 nmi to MAF-16A @ 10.5 kt	0.5	
MAF-16A	15°47.12'N	4511	Hole A - APC to 50 mbsf	0.0	1.1
EPSP	147°8.49'E		Hole B - APC to 50 mbsf	0.0	0.7
to 250 mbsf			Hole C - APC/XCB to 250 mbsf	0.0	3.0
			Subtotal days on-site: 4.8		
			Transit ~5 nmi to MAF-15A (drill-in reentry cone/casing option) @ 10.5 kt	0.0	
MAF-15A (drill-in reentry cone/casing option)	15°42.57'N	3677	Hole A - APC to 50 mbsf	0.0	1.0
EPSP	147°10.60'E		Hole B - APC to 50 mbsf	0.0	0.7
to 200 mbsf			Hole C - APC/XCB to 200 mbsf	0.0	2.3
			Hole D - Drill-in reentry cone w/casing to 200 mbsf/install bridge plug	0.0	4.5
			Subtotal days on-site: 8.5		
			Transit ~137 nmi to MAF-14A @ 10.5 kt	0.5	
MAF-14A	17°59.53'N	3267	Hole A - APC to 50 mbsf	0.0	1.0
EPSP	147°6.00'E		Hole B - APC to 50 mbsf	0.0	0.6
to 400 mbsf			Hole C - APC/XCB to 350 mbsf	0.0	3.1
			Subtotal days on-site: 4.7		
			Transit ~4 nmi to MAF-13A @ 10.5 kt	0.1	
MAF-13A	18°3.09'N	1411	Hole A - APC to 50 mbsf	0.0	0.7
EPSP	147°6.00'E		Hole B - APC to 50 mbsf	0.0	0.5
to 250 mbsf			Hole C - APC/XCB to 250 mbsf	0.0	1.9
			Subtotal days on-site: 3.1		
			Transit ~3 nmi to MAF-12B @ 10.5 kt	0.1	
MAF-12B	18°5.67'N	1411	Hole A - APC to 50 mbsf	0.0	0.7
EPSP	147°6.00'E		Hole B - APC to 50 mbsf	0.0	0.5
to 250 mbsf			Hole C - APC/XCB to 250 mbsf	0.0	1.9
			Subtotal days on-site: 3.1		
			Transit ~1 nmi to MAF-11A (drill-in reentry cone and casing option) @ 10.5 kt	0.1	
MAF-11A (drill-in reentry cone/casing option)	18°6.40'N	1260	Hole A - APC to 50 mbsf	0.0	0.7
EPSP	147°5.90'E		Hole B - APC to 50 mbsf	0.0	0.5
to 200 mbsf			Hole C - APC/XCB to 200 mbsf	0.0	1.6
			Hole D - Drill-in reentry cone w/casing to 200 mbsf/install bridge plug	0.0	4.0
			Subtotal days on-site: 6.8		
			Transit ~94 nmi to MAF-9B (drill-in reentry cone/casing option) @ 10.5 kt	0.4	
MAF-9B (drill-in reentry cone/casing option)	16°32.25'N	2011	Hole A - APC to 50 mbsf	0.0	0.8
EPSP	147°13.25'E		Hole B - APC to 50 mbsf	0.0	0.6
to 200 mbsf			Hole C - APC/XCB to 200 mbsf	0.0	1.9
			Hole D - Drill-In reentry cone w/casing to 200 mbsf/install bridge plug	0.0	4.1
			Subtotal days on-site: 7.3		
			Transit ~5 nmi to MAF-10B @ 10.5 kt	0.0	
MAF-10B	16°27.60'N	3211	Hole A - APC to 50 mbsf	0.0	1.0
EPSP	147°10.35'E		Hole B - APC to 50 mbsf	0.0	0.6
to 350 mbsf			Hole C - APC/XCB to 300 mbsf	0.0	3.0
			Subtotal days on-site: 4.6		
			Transit ~97 nmi to WP-06 @ 10.5 kt, ~1384 nmi to WP-07 @ 10.5 kt, and ~418 nmi to Hong Kong @ 10.5 kt	7.6	
Hong Kong			End expedition	9.7	46.3

Port call:	5.0	Total operating days:	56.0
Subtotal on-site:	46.3	Total expedition:	61.0

Figure F1. Color-contoured bathymetric map of the western Pacific showing the Mariana convergent margin system (large black box), drill site locations from Legs 125 and 195 (black lines), and locations of the three serpentinite mud volcanoes that will be cored during Expedition 366 (small boxes near the Mariana Trench). From north to south the target seamounts are: Big Blue Seamount (Sites MAF-11A, MAF-12B, MAF-13A, and MAF-14A), Celestial Seamount (Sites MAF-9B and MAF-10B), and Blue Moon Seamount (Sites MAF-15A and MAF-16A). During Leg 195, Hole 1200C on South Chamorro Seamount was cased and fitted with an original-style CORK, which will be refitted to accommodate a future CORK-Lite installation.

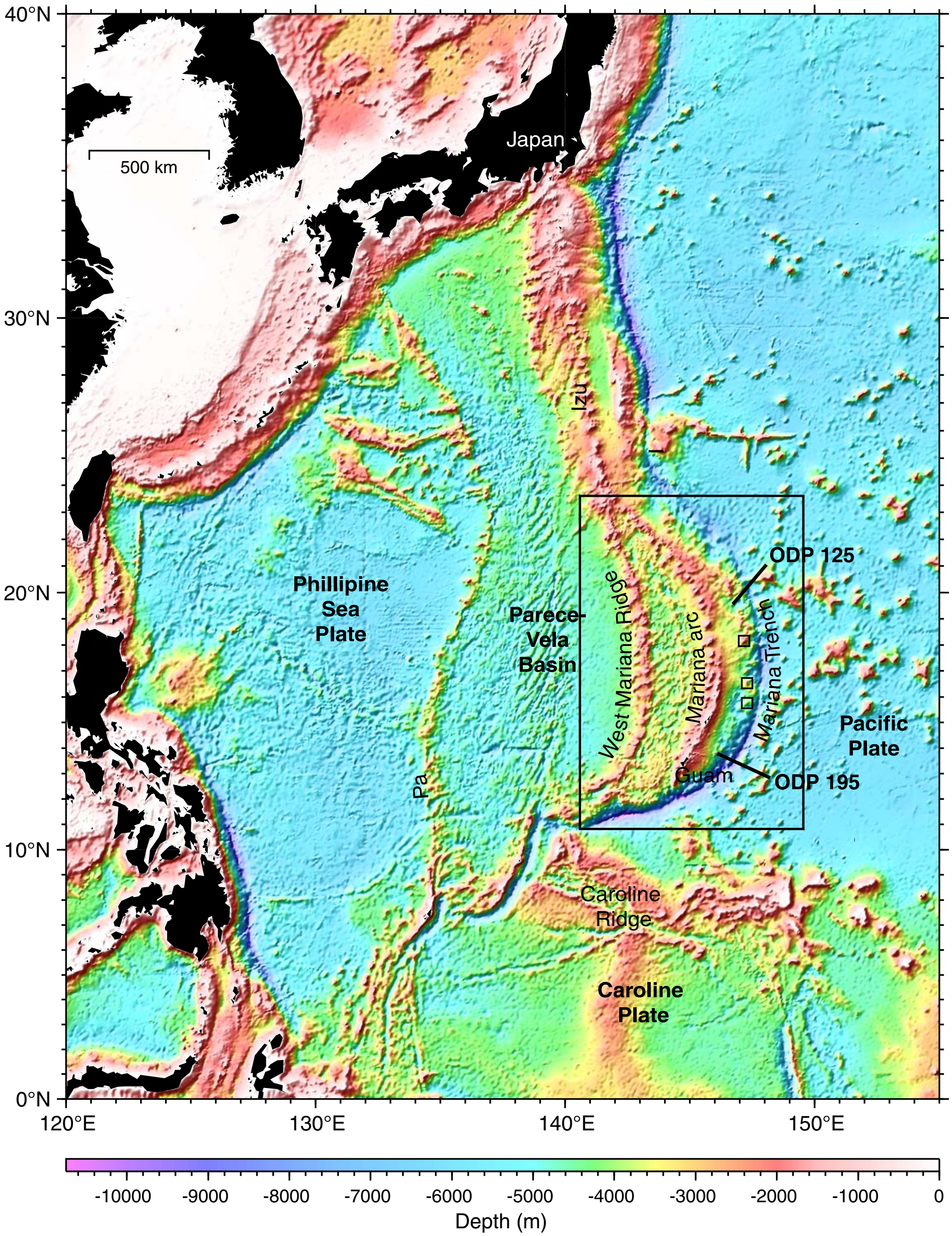

Figure F2. Mercator projection of the Mariana forearc. PSP = Philippine Sea plate, PP = Pacific plate, IBM = Izu-Bonin-Mariana Trenches, MT = Mariana Trough, WMR = West Mariana Ridge, PVB = Parece Vela Basin, PKR = Palau-Kushu Ridge, WPB = West Philippine Basin. Bathymetry of the central Mariana arc-trench system is from combined surveys, sunlit from the east, showing EW0202 cruise seismic lines. Pacific plate magnetic lineations from Nakanishi et al. (1992) are drawn in white. A, B, and C show locations for maps of Blue Moon, Big Blue, and Celestial Seamounts, respectively (Figures **AF1**, **AF5**, **AF8**). Data used are a combination of Hydrosweep data from EW0202/03 cruises, Simrad EM300 from a 2003 R/V *Thompson* cruise, 1997 HAWAII MR-1 data, and data from a composite of regional studies conducted on ships from the Japan Center for Marine Earth Science and Technology (N. Seama and M. Nakanishi, pers. comm., 2002). Bathymetric images are illuminated from the east to highlight relief. Lineations subparallel to ship tracks are data artifacts at the edges of bathymetry swaths resulting from different sound speed profiles used for adjacent data. (Modified from Oakley, 2008.)

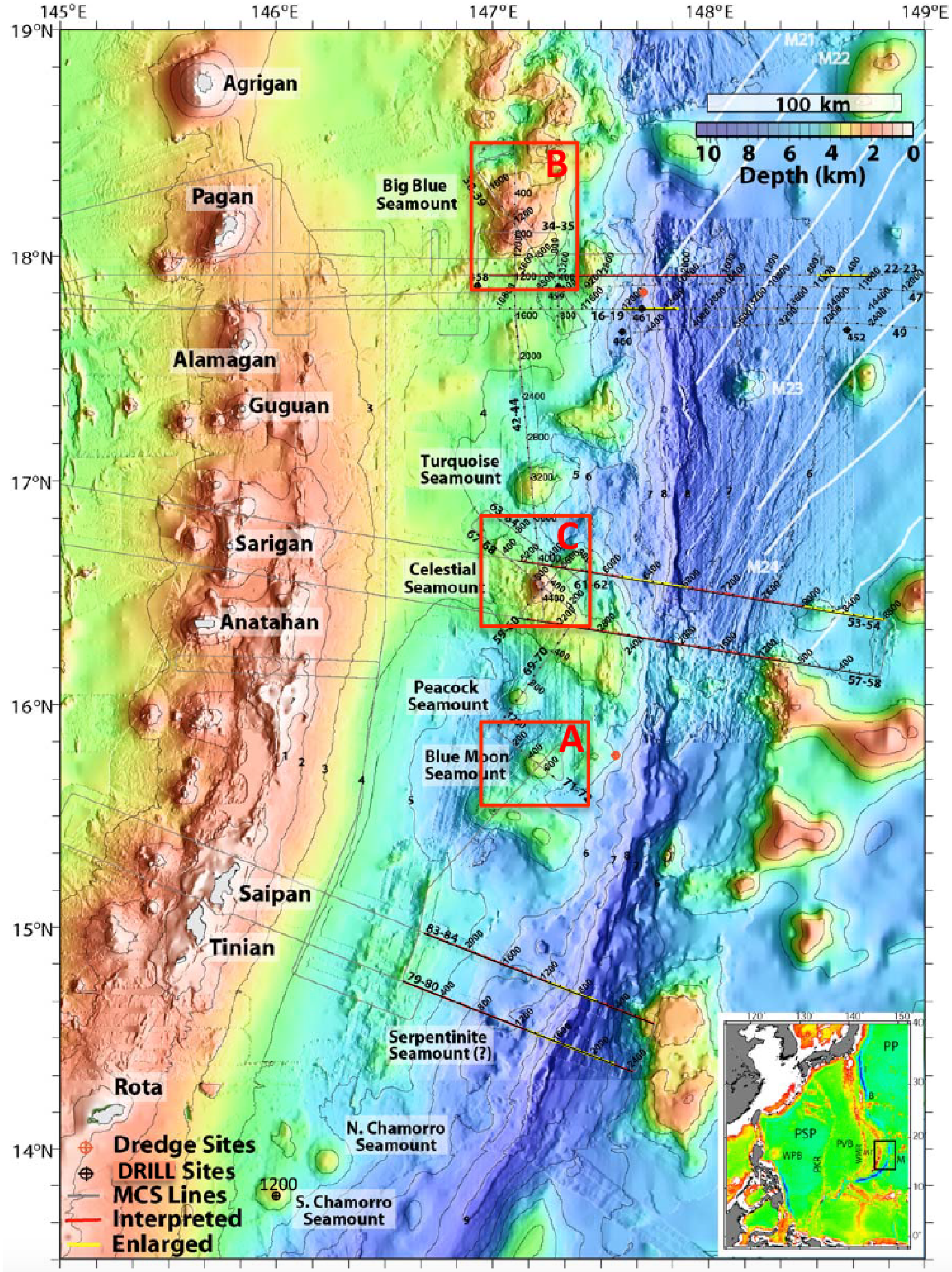

Figure F3. Schematic cross section of serpentinite mud volcano formation in the Mariana forearc. Extensive faulting resulting from regional tectonics creates conduits, particularly where faults intersect, and permits slab-derived fluids and serpentinized fault gouge of forearc mantle to rise, eventually reaching the seafloor. Fluid chemistry varies with the depth to the décollement. (Modified from Hulme et al., 2010.)

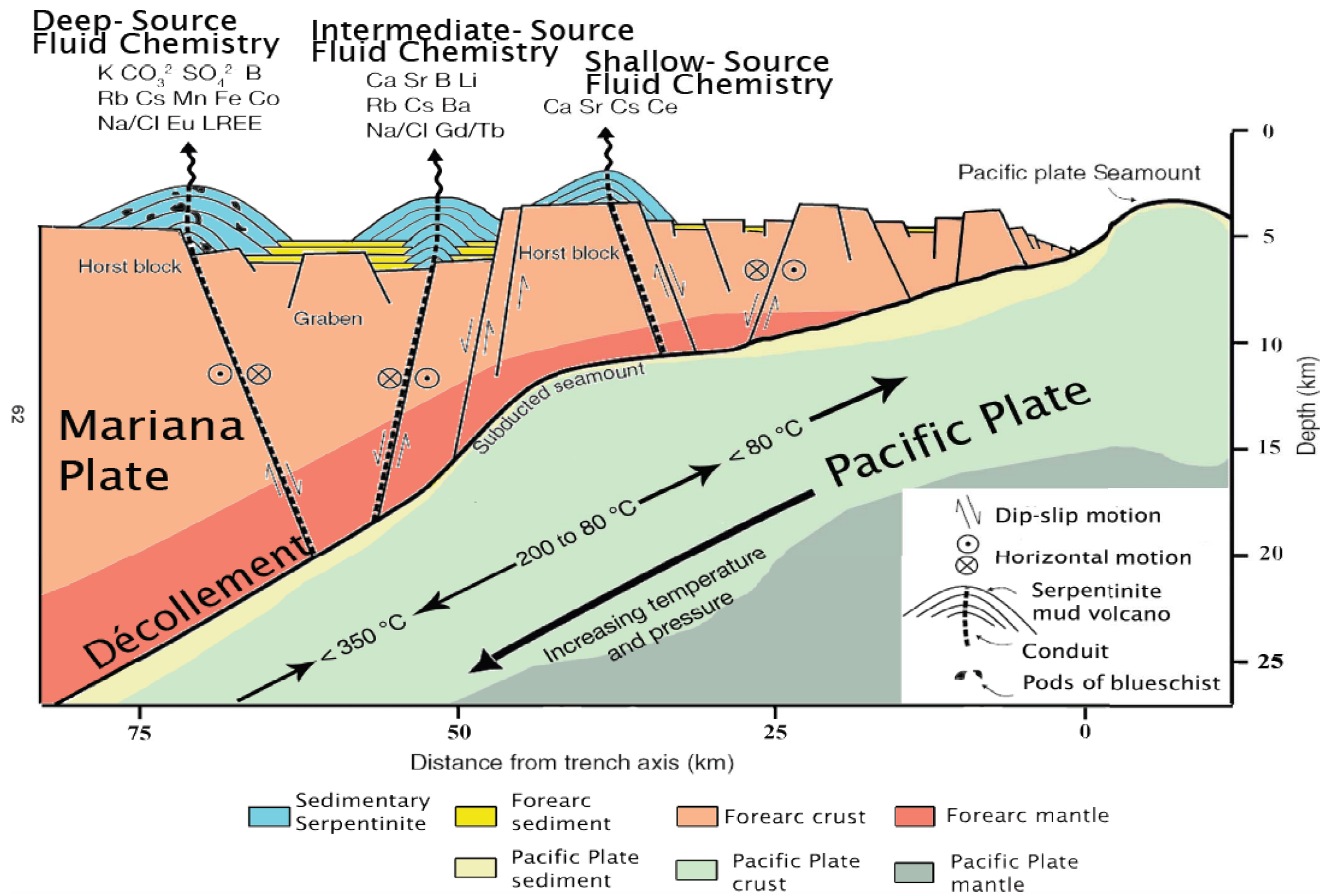

Figure F4. Top left: color-contoured EM 300 bathymetry map of Conical Seamount, showing locations of Sites 778, 779, and 780. Bottom left inset: perspective image of SeaMARK-II side-scan data (dark = high backscatter, rougher seafloor), looking from the south toward the north, showing locations of the three Leg 125 sites. VE = vertical exaggeration. Right: lithologic results of coring at these sites, but recovery was minimal because the serpentinite matrix is not well suited to rotary drilling (Fryer, Pearce, Stokking, et al., 1990).

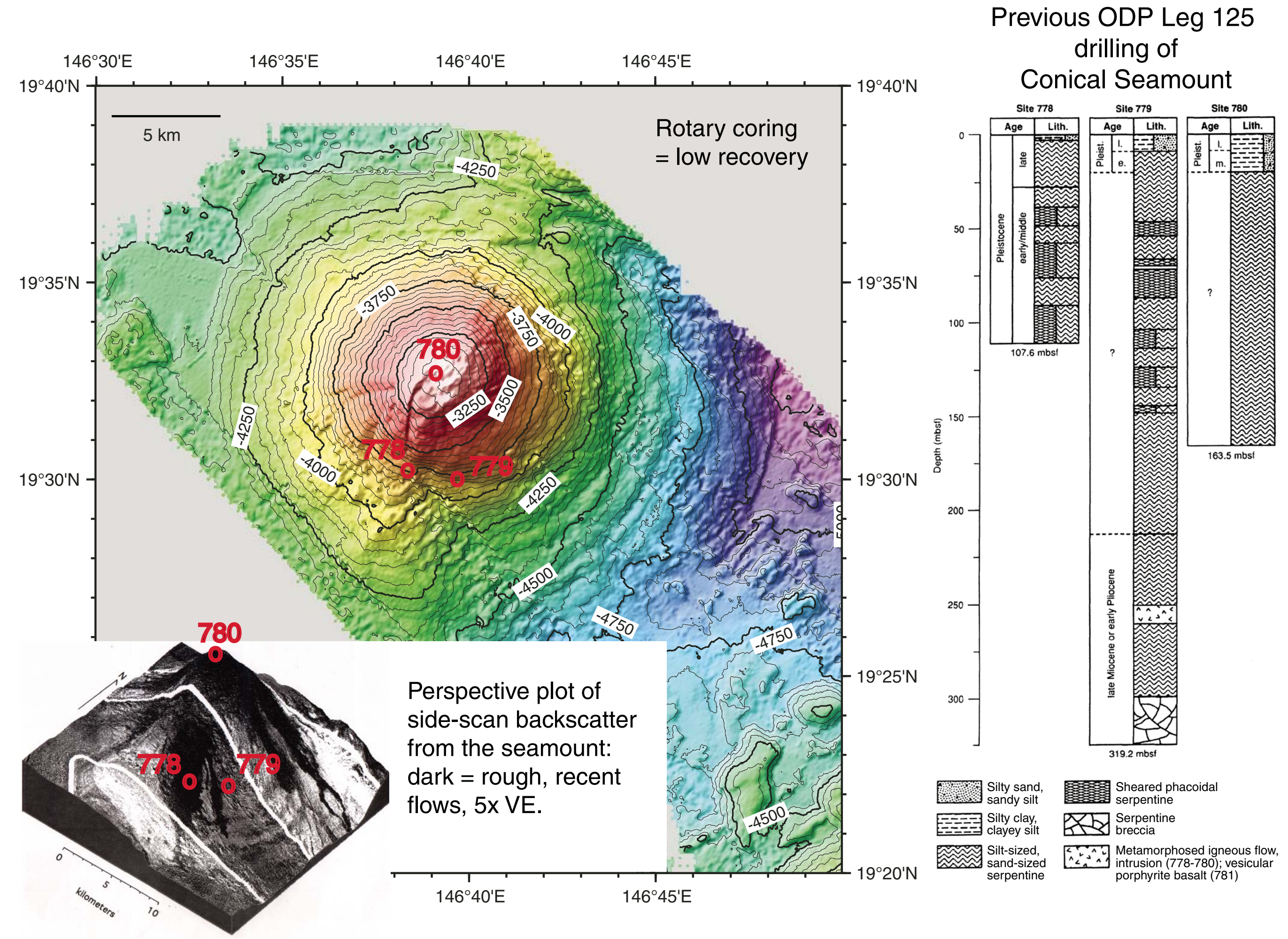

Figure F5. Upper right: color-contoured bathymetry data for South Chamorro Seamount, showing location of Hole 1200C (CORKed hole). Lower left: color-contoured image of summit area with DSL120 side-scan imagery superimposed on bathymetry, showing locations for all Site 1200 holes drilled on South Chamorro Seamount.

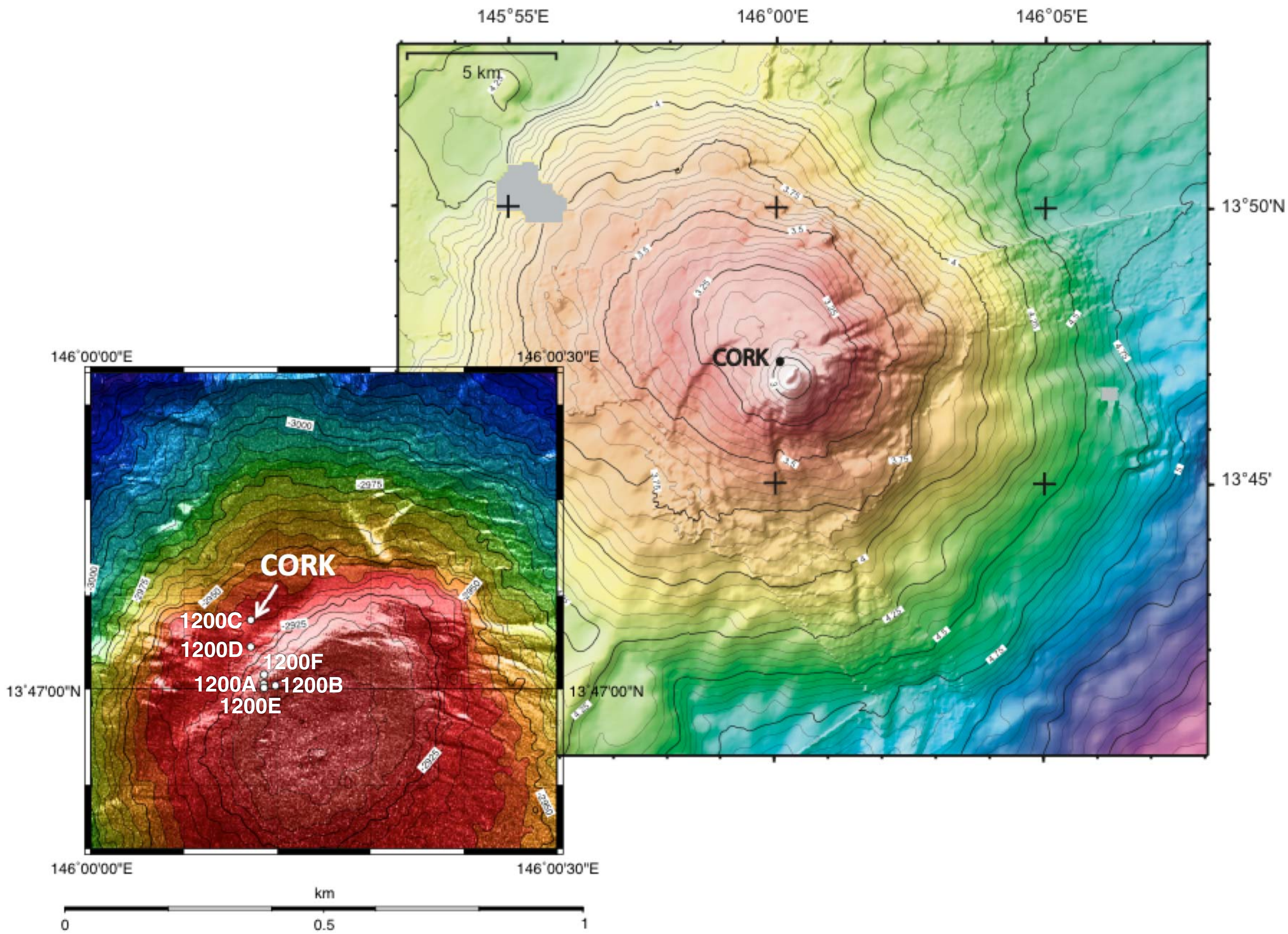

Site summaries

Site MAF-16A

Priority:	Primary
Position:	15°47.12′N, 147°8.49′E
Water depth (m):	4511
Target drilling depth (mbsf):	250
Approved maximum penetration (mbsf):	250
Survey coverage:	MCS Profile 71-72, common depth point (CDP) between 3121 and 3122 • Track map (Figures **AF1**, **AF2**) • Seismic profile (Figure **AF3**)
Objective(s):	Core Blue Moon Seamount northwest flank. Determine composition of slab-derived fluids and deep-derived metamorphosed rock materials and microbial populations. Determine age of any sediments encountered, the history of deformation, and the degree of serpentinization.
Drilling, coring, and downhole measurements program:	• Hole A: APC to 50 mbsf • Hole B: APC to 50 mbsf • Hole C: APC/XCB to 250 mbsf • Icefield MI-5 tool core orientation measurements • Formation temperature and pressure (APCT-3 and SETP/T2P)
Nature of rock anticipated:	Approximately 95% serpentinite mud with ~5% clasts of dominantly serpentinized peridotite and minor metabasite schists

Site MAF-15A

Priority:	Primary
Position:	15°42.57′N, 147°10.60′E
Water depth (m):	3677
Target drilling depth (mbsf):	200
Approved maximum penetration (mbsf):	100 (pending request to Environmental Protection and Safety Panel [EPSP] to deepen to 200 mbsf)
Survey coverage:	MCS Profile 71-72, at CDP 4432 (4.2 km southwest); MCS Profile 75-78, at CDP 3202 (1 km northwest) • Track map (Figures **AF1**, **AF2**) • Seismic profile (Figures **AF3**, **AF4**)
Objective(s):	Core Blue Moon Seamount summit, including fluid conduit. Install infrastructure for future CORK-Lite deployment. Determine composition of slab-derived fluids and deep-derived metamorphosed rock materials and microbial populations. Determine the history of deformation and the degree of serpentinization.
Drilling, coring, and downhole measurements program:	• Hole A: APC to 50 mbsf • Hole B: APC to 50 mbsf • Hole C: APC/XCB to 200 mbsf • Icefield MI-5 tool core orientation measurements • Formation temperature and pressure (APCT-3 and SETP/T2P)
Nature of rock anticipated:	Approximately 95% serpentinite mud with ~5% clasts of dominantly serpentinized peridotite and minor metabasite schists

Site MAF-14A

Priority:	Primary
Position:	17°59.53′N, 147°6.00′E
Water depth (m):	3267
Target drilling depth (mbsf):	350
Approved maximum penetration (mbsf):	250 (pending request to EPSP to deepen to 350 mbsf)
Survey coverage:	MCS Profile 42-44, CDP 8679 • Track map (Figure **AF5**) • Seismic profile (Figures **AF6**, **AF7**)
Objective(s):	Core Big Blue Seamount south flank at toe of slope. Determine composition of slab-derived fluids and deep-derived metamorphosed rock materials and microbial populations. Determine the history of deformation and the degree of serpentinization. Core sedimentary strata underlying the mud volcano and the interface between the two.
Drilling, coring, and downhole measurements program:	• Hole A: APC to 50 mbsf • Hole B: APC to 50 mbsf • Hole C: APC/XCB to 350 mbsf • Icefield MI-5 tool core orientation measurements • Formation temperature and pressure (APCT-3 and SETP/T2P) • Downhole logging is not planned, but this site has the deepest penetration of the expedition and is the most likely to have a stable open borehole. Logging might be possible here if time is available.
Nature of rock anticipated:	Mud volcano: ~95% serpentinite mud with ~5% clasts of dominantly serpentinized peridotite and minor blueschist facies metabasite Underlying sedimentary rocks: vitric silt, Eocene to Pleistocene in age(?)

Site MAF-13A

Priority:	Primary
Position:	18°3.09′N, 147°6.00′E
Water depth (m):	2200
Target drilling depth (mbsf):	250
Approved maximum penetration (mbsf):	250
Survey coverage:	MCS Profile 42-44, CDP 7631 • Track map (Figure **AF5**) • Seismic profile (Figures **AF6**, **AF7**)
Objective(s):	Core Big Blue Seamount south flank. Determine composition of slab-derived fluids and deep-derived metamorphosed rock materials and microbial populations. Determine the history of deformation and the degree of serpentinization.
Drilling, coring, and downhole measurements program:	• Hole A: APC to 50 mbsf • Hole B: APC to 50 mbsf • Hole C: APC/XCB to 250 mbsf • Icefield MI-5 tool core orientation measurements • Formation temperature and pressure (APCT-3 and SETP/T2P)
Nature of rock anticipated:	Mud volcano: ~95% serpentinite mud with ~5% clasts of dominantly serpentinized peridotite and minor metabasite schists

Site MAF-12B

Priority:	Primary
Position:	18°5.67′N, 147°6.00′E
Water depth (m):	1403
Target drilling depth (mbsf):	250
Approved maximum penetration (mbsf):	250
Survey coverage:	MCS Profile 42-44, CDP between 6860 and 6870 • Track map (Figure **AF5**) • Seismic profile (Figures **AF6**, **AF7**)
Objective(s):	Core Big Blue Seamount summit south side. Determine composition of slab-derived fluids and deep-derived metamorphosed rock materials and microbial populations. Determine the history of deformation and the degree of serpentinization.
Drilling, coring, and downhole measurements program:	• Hole A: APC to 50 mbsf • Hole B: APC to 50 mbsf • Hole C: APC/XCB to 250 mbsf • Icefield MI-5 tool core orientation measurements • Formation temperature and pressure (APCT-3 and SETP/T2P)
Nature of rock anticipated:	Mud volcano: ~95% serpentinite mud with ~5% clasts of dominantly serpentinized peridotite and minor metabasite schists

Site MAF-11A

Priority:	Primary
Position:	18°6.40′N, 147°5.90′E
Water depth (m):	1260
Target drilling depth (mbsf):	200
Approved maximum penetration (mbsf):	150 (pending request to EPSP for approval for 200 mbsf)
Survey coverage:	MCS Profile 42-44, CDP 6653 • Track map (Figure **AF5**) • Seismic profile (Figures **AF6**, **AF7**)
Objective(s):	Core Big Blue Seamount summit, including fluid conduit. Install infrastructure for future CORK-Lite deployment. Determine composition of slab-derived fluids and deep-derived metamorphosed rock materials and microbial populations. Determine the history of deformation and the degree of serpentinization.
Drilling, coring, and downhole measurements program:	• Hole A: APC to 50 mbsf • Hole B: APC to 50 mbsf • Hole C: APC/XCB to 200 mbsf • Icefield MI-5 tool core orientation measurements • Formation temperature and pressure (APCT-3 and SETP/T2P)
Nature of rock anticipated:	Mud volcano: ~95% serpentinite mud with ~5% clasts of dominantly serpentinized peridotite and minor metabasite schists

Site MAF-9B

Priority:	Primary
Position:	16°32.25′N, 147°13.25′E
Water depth (m):	2011
Target drilling depth (mbsf):	200
Approved maximum penetration (mbsf):	150 (pending request to EPSP for approval for 200 mbsf)
Survey coverage:	MCS profile 42-44, CDP 34602 • Track map (Figure **AF8**) • Seismic profile (Figures **AF9**, **AF10**, **AF11**)
Objective(s):	Core Celestial Seamount summit. Install infrastructure for future CORK-Lite deployment. Determine composition of slab-derived fluids and deep-derived metamorphosed rock materials and microbial populations. Determine the history of deformation and the degree of serpentinization.
Drilling, coring, and downhole measurements program:	• Hole A: APC to 50 mbsf • Hole B: APC to 50 mbsf • Hole C: APC/XCB to 200 mbsf • Icefield MI-5 tool core orientation measurements • Formation temperature and pressure (APCT-3 and SETP/T2P)
Nature of rock anticipated:	Mud volcano: ~95% serpentinite mud with ~5% clasts of dominantly serpentinized peridotite and minor metabasite schists

Site MAF-10B

Priority:	Primary
Position:	16°27.6′N, 147°10.35′E
Water depth (m):	3211
Target drilling depth (mbsf):	300
Approved maximum penetration (mbsf):	250 (pending request to EPSP for approval for 300 mbsf or deeper)
Survey coverage:	MCS Profile 59-60, CDP 1561 • Track map (Figure **AF8**) • Seismic profile (Figure **AF10**)
Objective(s):	Core Celestial Seamount southwest flank. Determine composition of slab-derived fluids and deep-derived metamorphosed rock materials and microbial populations. Determine the history of deformation and the degree of serpentinization.
Drilling, coring, and downhole measurements program:	• Hole A: APC to 50 mbsf • Hole B: APC to 50 mbsf • Hole C: APC/XCB to 300 mbsf (may extend deeper if time at end of expedition but would need EPSP approval) • Icefield MI-5 tool core orientation measurements • Formation temperature and pressure (APCT-3 and SETP/T2P)
Nature of rock anticipated:	Mud volcano: ~95% serpentinite mud with ~5% clasts of dominantly serpentinized peridotite and minor metabasite schists

Appendix

Bathymetry and MCS data for Expedition 366 target sites

In February and March of 2002 an MCS survey was conducted of the central Mariana arc system using the R/V *Maurice Ewing* towing a 6 km 480 channel streamer cable (Oakley et al., 2007). Shots were fired every 50 m from a tuned 6817 cubic inch array of 20 air guns. The data were recorded in SEG-D format, with a sampling interval of 2 µs. At sea, resampling to 4 µs, application of geometry, trace editing, velocity analysis, inside and outside mutes, stacking, and time migration were completed. Additional shore-based processing designed to enhance reflections and remove multiples included methods such as Radon velocity filtering, F-K filtering, and deconvolution. The data were deconvolved prior to stacking in order to remove false seafloor parallel reflections created by the air gun bubble pulse. This technique, although successful, had the undesirable effect of partially suppressing the real reflections, resulting in a low-amplitude band just below the seafloor. The PROMAX 2-D processing sequence applied to all lines was as follows:

1. Resample to 4 ms
2. Edit bad traces
3. Geometry
4. Sort to common midpoint gathers (CMP) at 6.25 m
5. Bandpass filter (4-6-60-70 Hz)
6. Velocity analysis
7. Normal moveout correction
8. Top mute
9. Bottom mute
10. Prestack deconvolution (to remove air gun bubble pulse)
11. Radon velocity filter
12. CMP ensemble stack
13. Windowed F-K filter below multiple
14. Bottom mute just above multiple
15. Stolt F-K time migration
16. Automatic gain control
17. Time-varying bandpass filter
18. Postmigration depth conversion
19. Top mute for display

The seismic lines presented in this report were time migrated after muting the seafloor multiple then converted to depth (except for Line 67-68). Interval velocities used in these conversions were based on data from drill sites in the forearc region (ODP Hole 783A and Site 779), refraction data, and corrections for velocity "pullup" (Oakley et al., 2007).

Bathymetry data and MCS profiles for drilling target sites are provided in the appendix figures.

Figure AF1. Bathymetry maps of A on Figure **F1**, Blue Moon Seamount (Mercator projection, depth annotations every 1000 m). Left: color-contoured map is illuminated from the east. Right: map is contoured at 100 m intervals and annotated every 1000 m. Seismic lines are shown on Figures **AF3** and **AF4**.

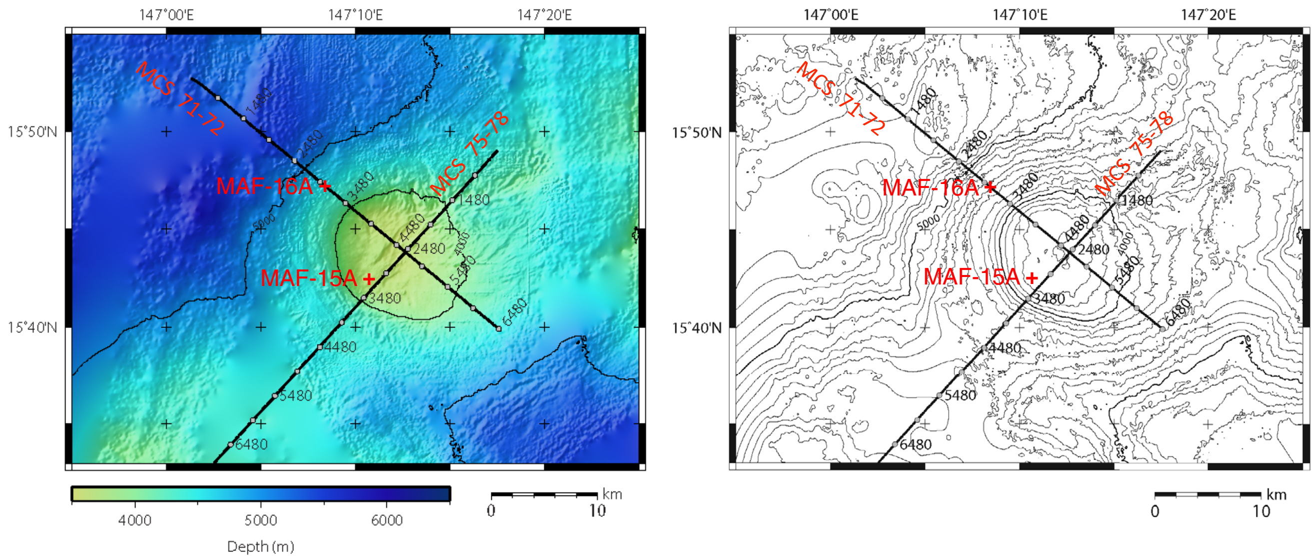

Figure AF2. Side-scan sonar backscatter image, Blue Moon Seamount summit area. Dark areas indicate areas of rough seafloor and/or scarps. Track nadir is at 15°45′N, and artifacts there are due to cross talk between the 11 and 12 kHz acoustic arrays. The dark area at proposed Site MAF-15A is an active spring visited in 2003 with the *Jason-2* ROV. This was the rationale for choosing this site off of MCS Line 75-78.

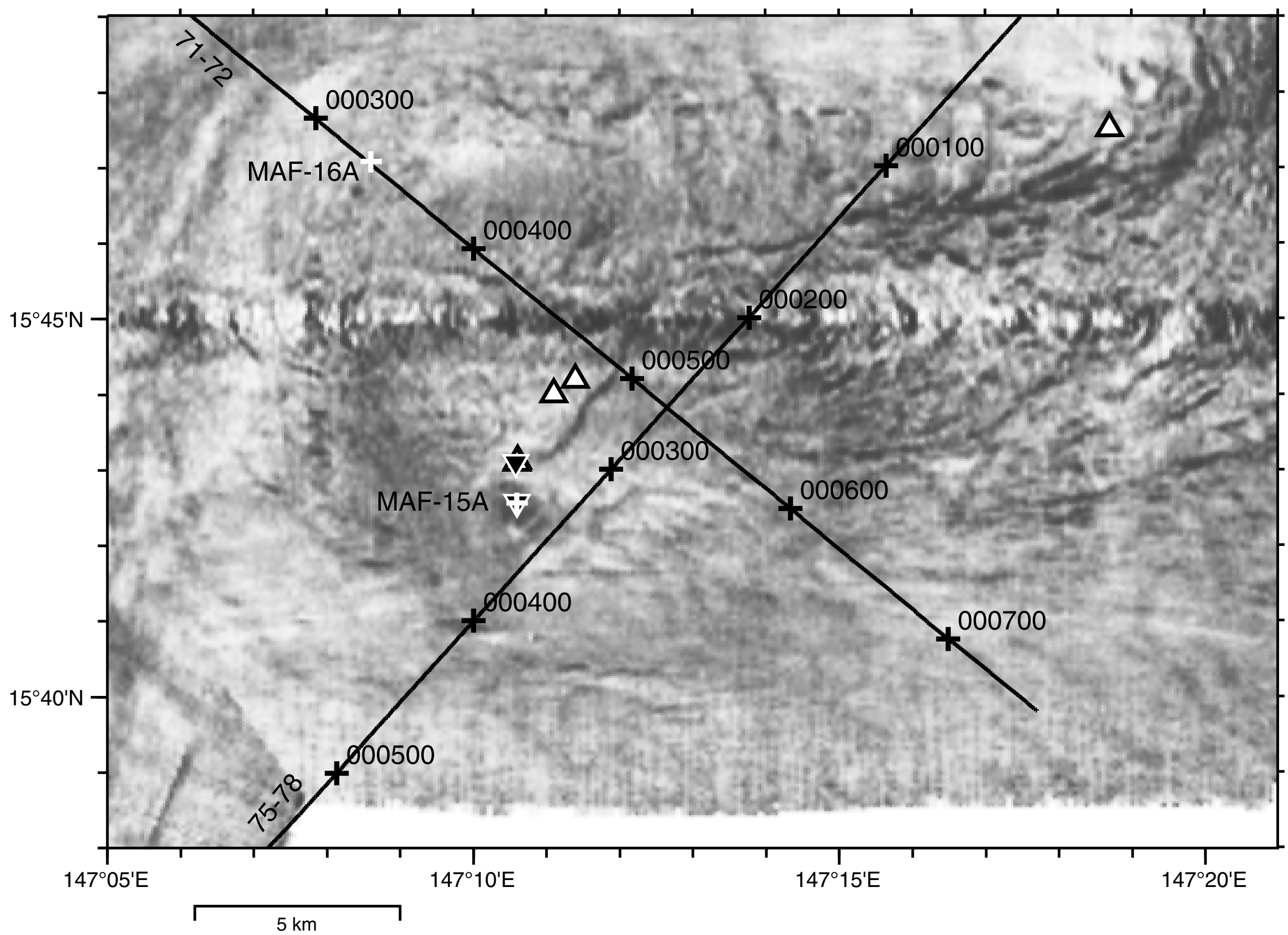

Figure AF3. Ewing 0202 cruise MCS Line 71-72 across Blue Moon Seamount proposed Sites MAF-15A and MAF-16A. Location of line and site shown on Figure **AF1**.

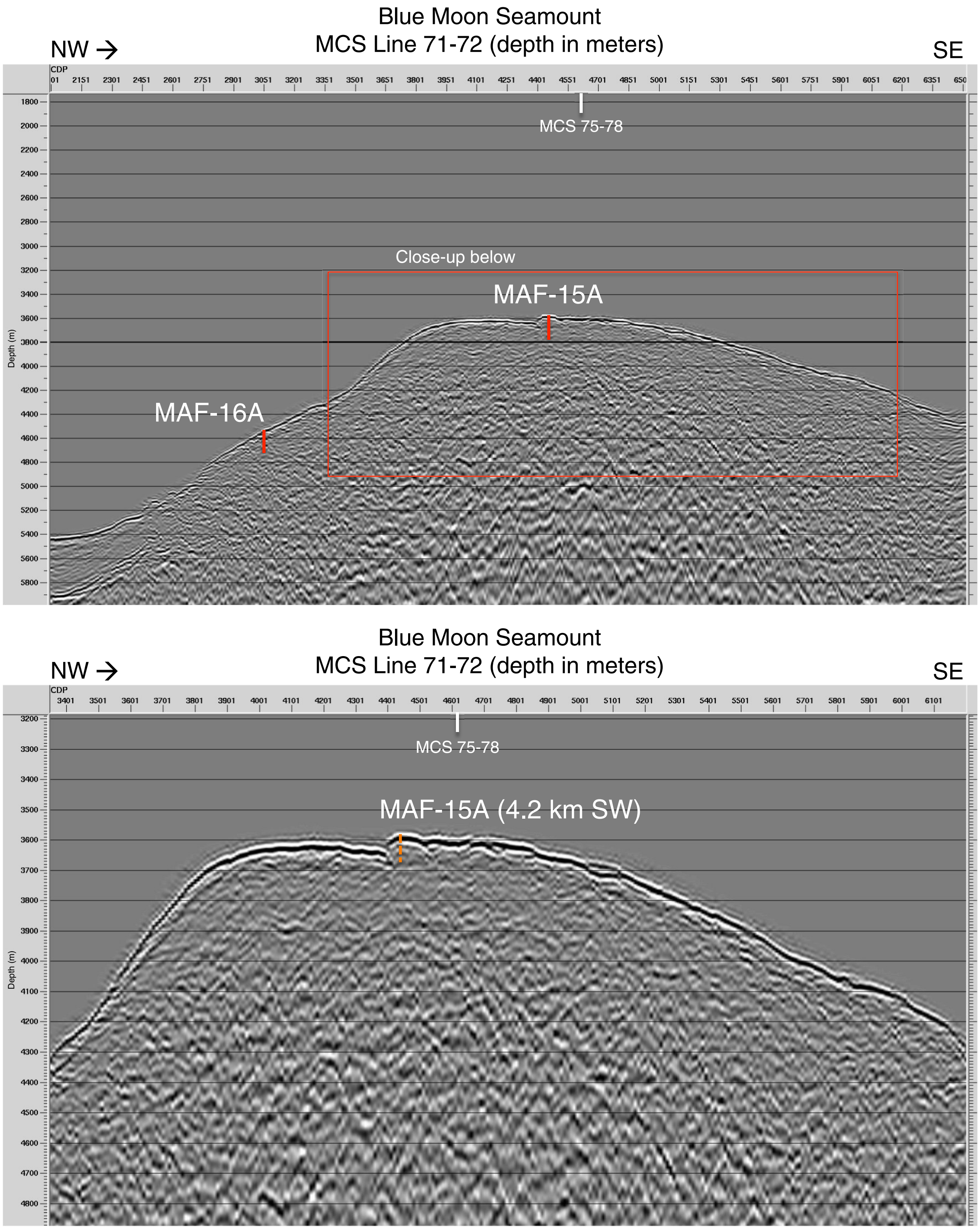

Figure AF4. Ewing 0202 cruise MCS Line 75-78 near Blue Moon Seamount proposed Site MAF-15A, which lies 1 km northwest. Location of line and site shown on Figure **AF1**.

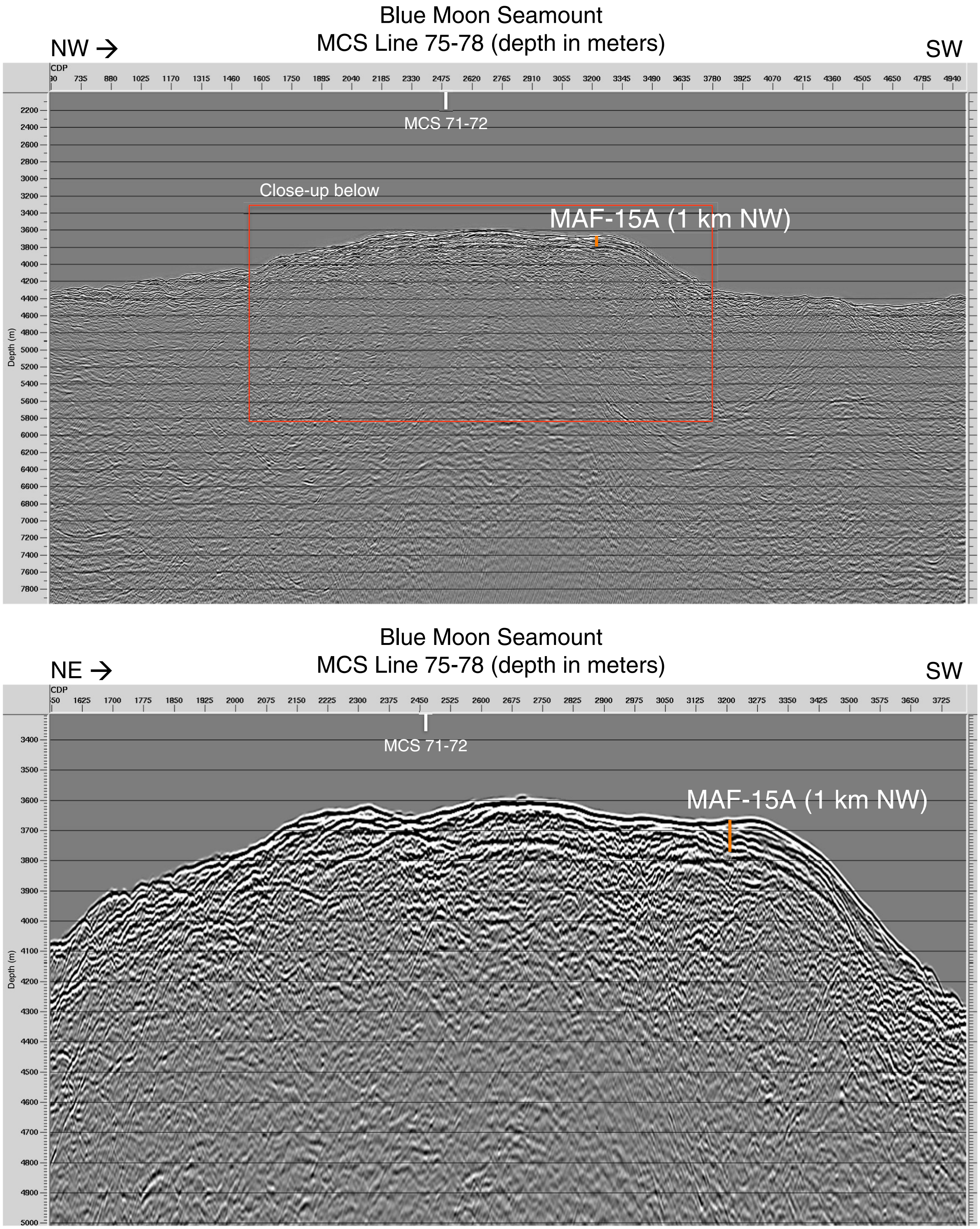

Figure AF5. Bathymetry maps of B on Figure **F1**, Big Blue Seamount (Mercator projection, depth annotations every 1000 m). Left: color-contoured map is illuminated from the east. Right: map is contoured at 100 m intervals and annotated every 1000 m. Seismic lines are shown on Figures **AF6** and **AF7**.

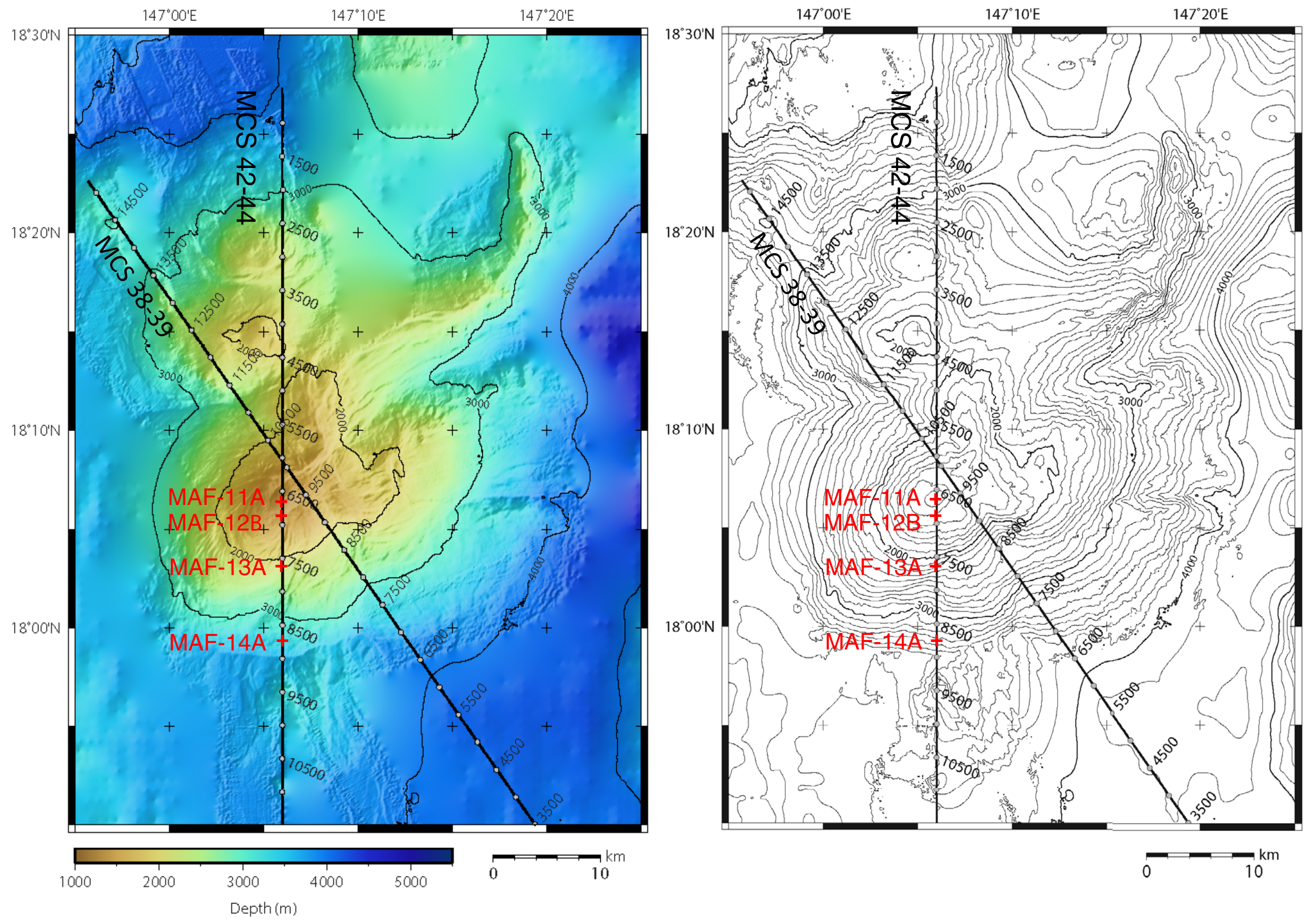

Figure AF6. Ewing 0202 cruise MCS Line 42-44 across Big Blue Seamount proposed Sites MAF-11A, MAF-12B, MAF-13A, and MAF-14A. Location of line and sites shown on Figure **AF5**.

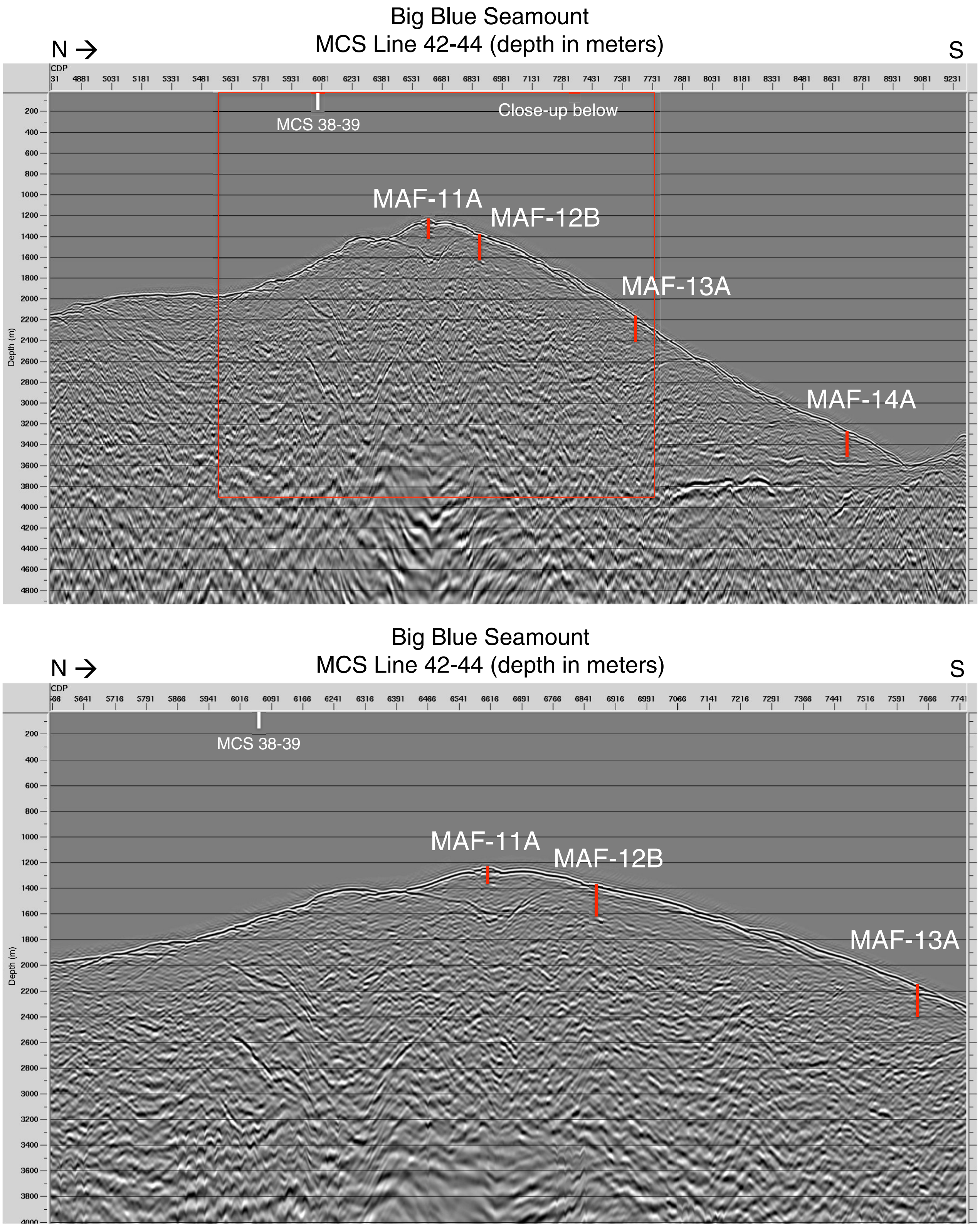

Figure AF7. Ewing 0202 cruise MCS Line 38-39 across Big Blue Seamount. Proposed Sites MAF-11A, MAF-12B, MAF-13A, and MAF-14A lie off this profile to the south. Location of line and sites shown on Figure **AF5**.

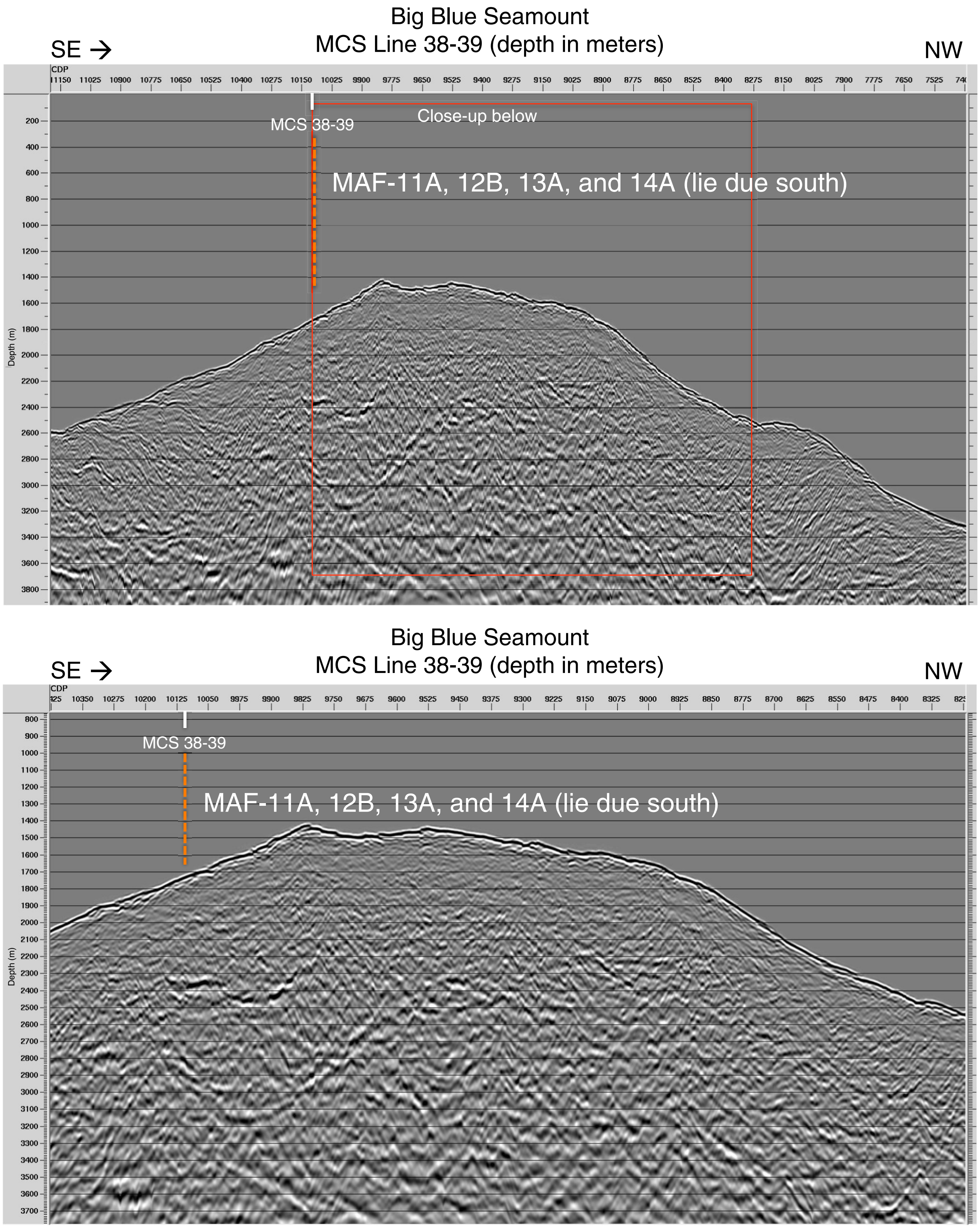

Figure AF8. Bathymetry maps of A on Figure **F1**, Celestial Seamount (Mercator projection, depth annotations every 1000 m). Left: color-contoured map is illuminated from the east. Right: map is contoured at 100 m intervals and annotated every 1000 m. Seismic lines are shown on Figures **AF9**, **AF10**, and **AF11**.

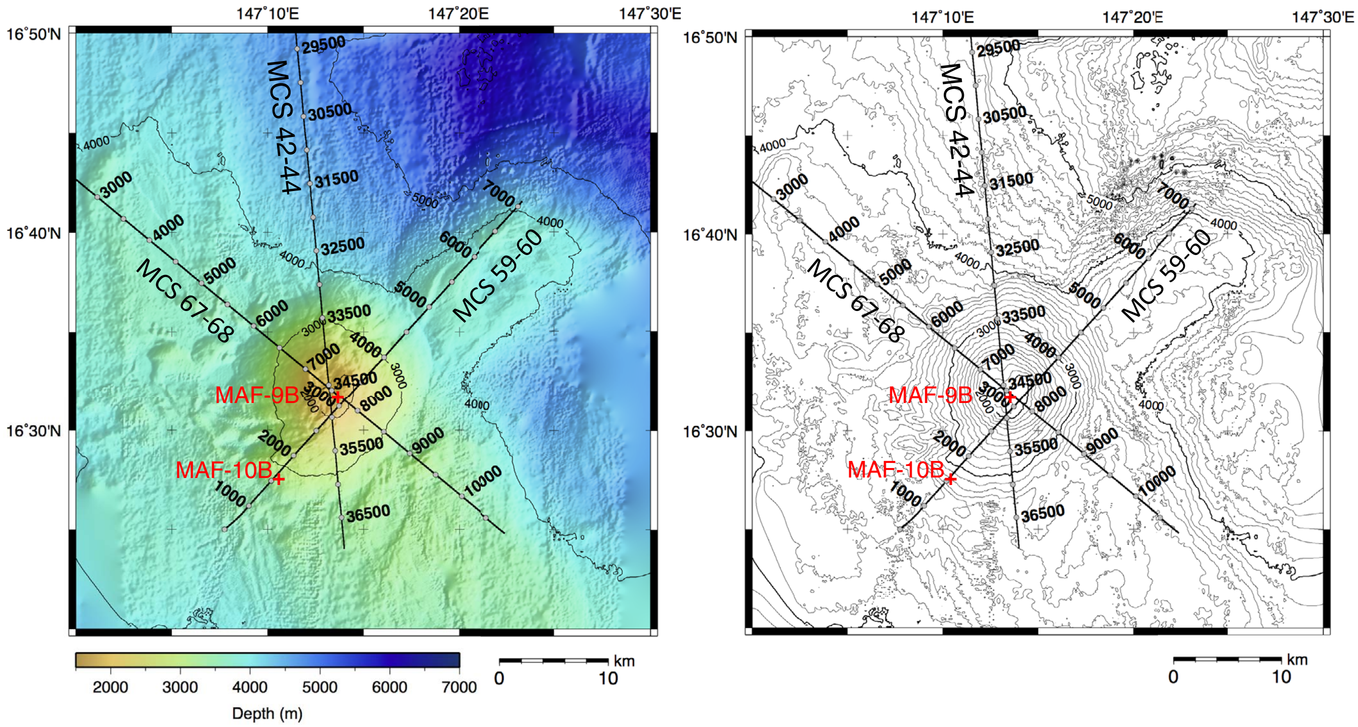

Figure AF9. Ewing 0202 cruise MCS Line 42-44 near Celestial Seamount proposed Site MAF-9B. Location of line and site shown on Figure **AF8**.

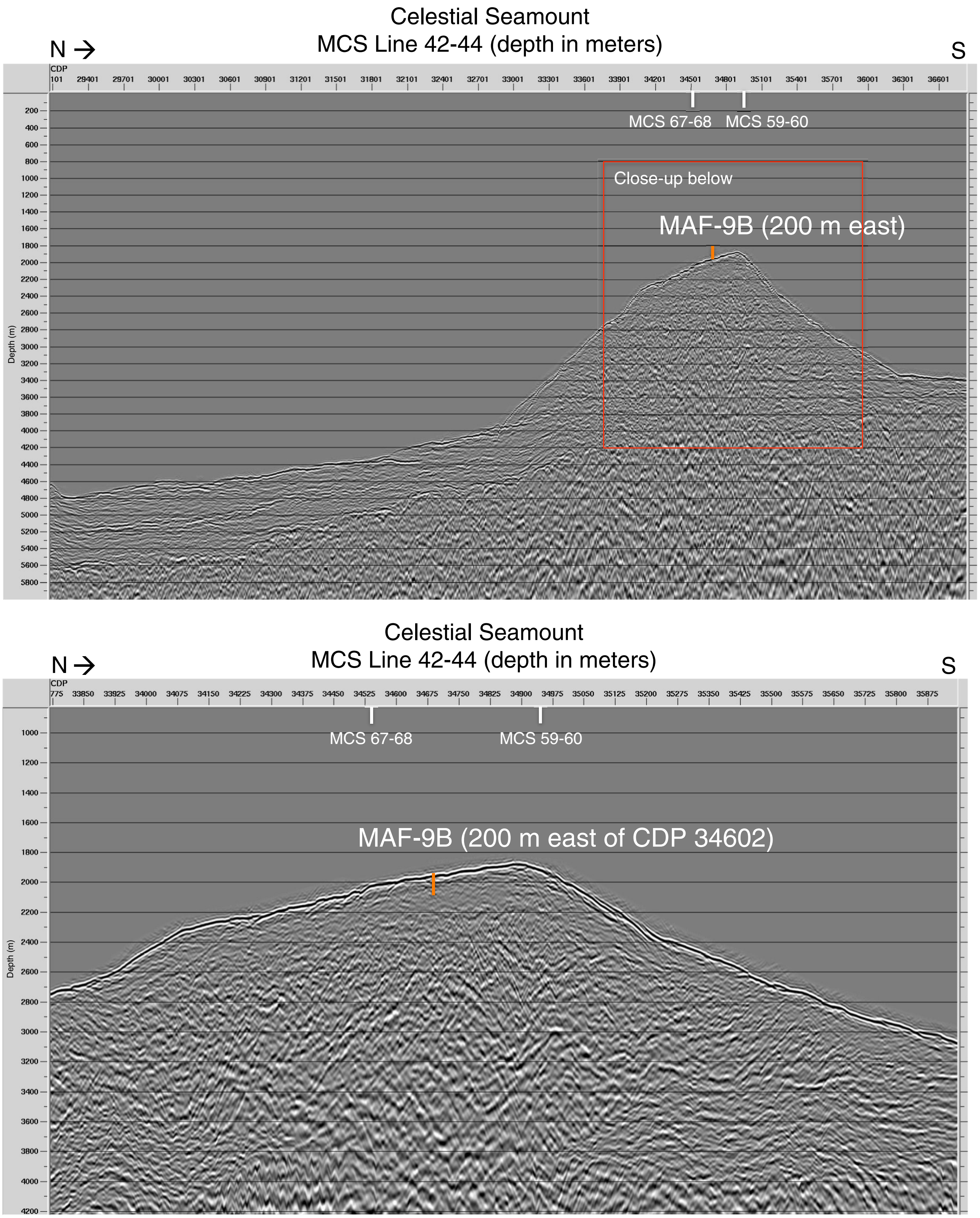

Figure AF10. Ewing 0202 cruise MCS Line 59-60 across Celestial Seamount proposed Site MAF-10B and south of proposed Site MAF-9B. Location of line and sites shown on Figure **AF8**.

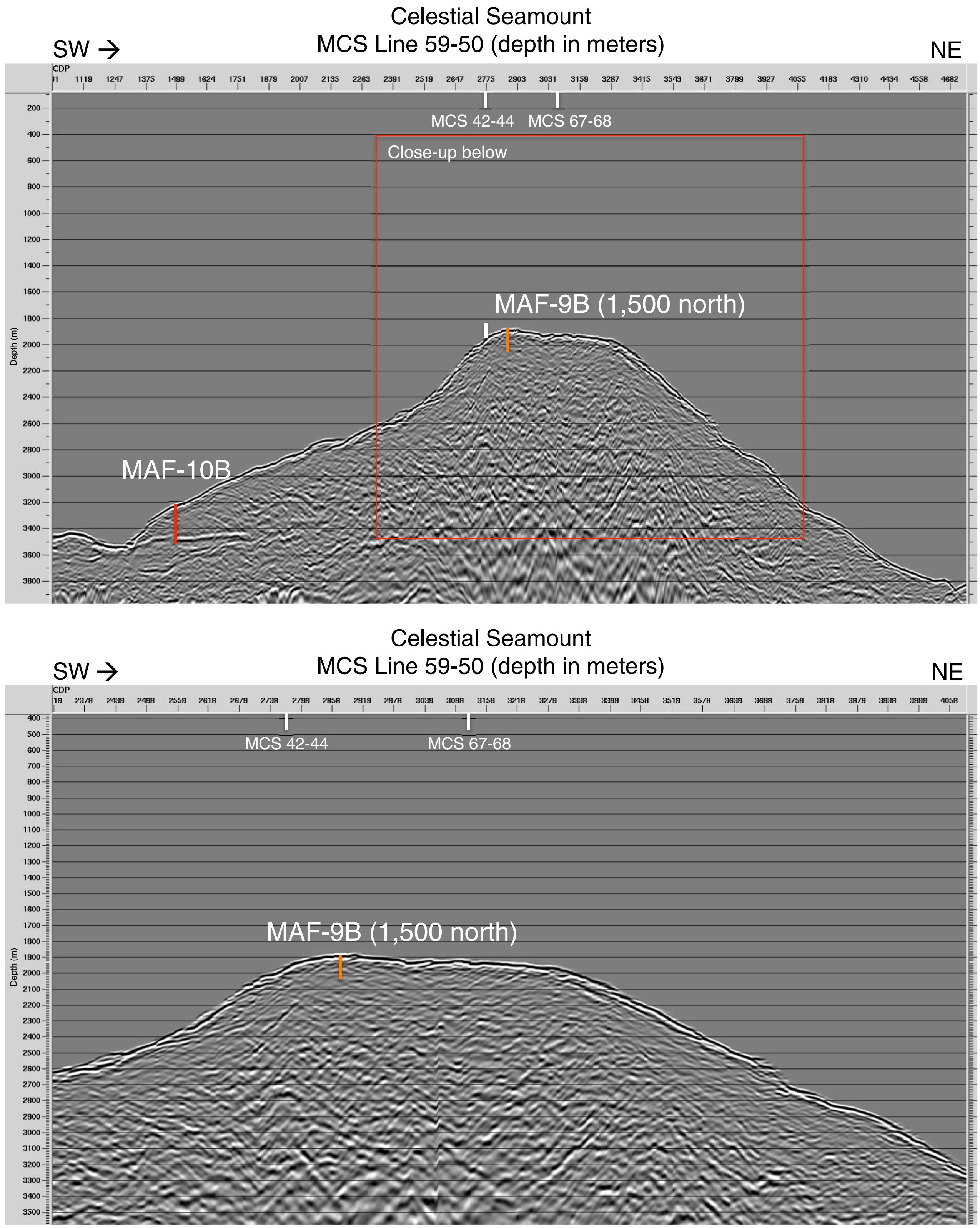

Figure AF11. Ewing 0202 cruise MCS Line 67-68 near Celestial Seamount proposed Site MAF-9B. Location of line and site shown on Figure **AF8**.